GEOMAGNETIC FIELD VARIATIONS AT AFRICAN EQUATORIAL REGIONS DURING THE ASCENDING PHASE OF THE SOLAR CYCLE 24

BY

LUCY ATIENO OBUYA

A THESIS SUBMITTED IN PARTIAL FULFILMENT OF THE REQUIREMENTS FOR THE DEGREE OF MASTER OF SCIENCE IN PHYSICS

SCHOOL OF PHYSICAL AND BIOLOGICAL SCIENCES

MASENO UNIVERSITY

DECLARATION

This thesis is my personal work and has not been submitted or presented for award of any degree to any university.

OBUYA LUCY ATIENO

MSC/SC/00014/2017

Signature…… Date…….

This thesis has been presented with our approval as supervisors.

DR. GEORGE OMONDI

Department of Physics and Materials Science

Maseno University

P.O Box 333-40105,

MASENO, KENYA

Signature…….. Date…….

PROF. ANDREW ODUOR

Department of Physics and Materials Science

Maseno University

P.O Box 333-40105

MASENO, KENYA

Signature…… Date…….

ACKNOWLEDGEMENT

This work has been made successful through the constant guidance and sincere corrections from my supervisors; Dr. Omondi George and Prof. Oduor Andrew, who dedicated their time to work with me. I therefore appreciate their effort in making it successful. My Spouse, Mr. Wayumba and my entire family, for supporting me morally, spiritually and financially and for encouraging me constantly through this work. My friend and colleague, Dr.Valence Habyarimana of Mbarara University of Science and Technology for his immense support and technical advice. The physics laboratory technicians and the departmental staff that were always available to assist whenever there was need and the Maseno University administration that gave me an opportunity to carry out this work. Finally I am indebted to the International Real-time Magnetic Observatory Network (INTERMAGNET) and African Meridian B-field Education and Research (AMBER) teams for availing the magnetometer data resources that were used in this work.

DEDICATION

Dedicated to my parents for the effort they put in ensuring I got the basic education which laid a solid foundation for this work.

ABSTRACT

The Earth's magnetic field is the field of force that extends from the interior of the Earth to the outer space where it interconnects with the Interplanetary Magnetic Field (IMF). It is characterized by regular and irregular variations. Previous researches have shown the geomagnetic field variations at different sectors of the world. Despite the significance of knowledge on geomagnetic field variations to industry, communication and navigation as well as the localized nature of ionospheric dynamics, geomagnetic field variation studies in Africa is still not fully exploited. Therefore, knowledge gaps that this study has bridged are: the solar quiet seasonal and annual variations; the seasonal and annual variations of Equatorial Electrojet current (EEJ) strength as well as the storm time variations of the Earth's magnetic field in the African equatorial regions during the ascending phase of the 24^{th} solar cycle, comparing different stations within the African equatorial region. Based on the aforementioned knowledge gaps, the problem of this study was the little accessible information on the Geomagnetic field variations in the African equatorial region during the ascending phase of solar cycle 24 from the year 2009-2014 to help establish its solar quiet and storm time variations in Addis Ababa, Adigrat, Mbour and Yaoundé stations and to estimate the EEJ strength in Mbour and Addis Ababa for the period 2009 to 2014 for identification of the specific and unique trends within this region, that may be useful for industries and space agencies in the region for purposes of planning and preparations for space weather eventualities. The objectives set to be achieved by this study were: to establish the solar quiet seasonal and annual variations of Earth's magnetic field; to determine the storm time variations of the geomagnetic field at Adigrat (ETHI) , Addis Ababa(AAE), Yaoundé(CMRN) and Mbour(MBO) during the Ascending phase of the solar cycle 24 from the year 2009 to 2014; and to estimate the seasonal and annual Equatorial Electrojet (EEJ) strength at Addis Ababa and Mbour for the period from 2009 to 2014. The Solar quiet (Sq) variations were calculated by method of non-cyclic variation and EEJ strength estimated using the two station method. The monthly values were averaged for months in a season to give seasonal variations while the average monthly values for a particular year provided the annual variations. The storm perturbations were obtained by subtracting the Sq of the most quiet day of every month from the Storm time variation of that day under study. Sq showed a seasonal variation which recorded the highest magnitudes of 110nT, 70nT, 65nT and 75nT for AAE, CMRN, ETHI and MBO respectively in the Equinoxes and lowest magnitudes of 50nT, 40nT, 40nT and 45nT for AAE, CMRN, ETHI and MBO respectively during the June solstices. Both the annual and seasonal variations showed solar activity, longitude and the local time dependence. The seasonal and annual variations in the EEJ strength showed larger magnitudes at Addis Ababa as compared to Mbour but larger peaks of westward Counter Electrojet (CEJ) current in Mbour as compared to Addis Ababa. The EEJ annual variation peaks during low solar activity years occurred earlier at about 1200LT as compared to peaks during high solar activity years which occurred between 1300LT and 1400LT, an outcome attributed to earlier ionization peaks during low solar activity leading to increased ionospheric conductivity. The storm time variation had a latitudinal variation. The results are useful for long term forecasting on the impact of geomagnetic field variations to help mitigate the effects of storms on the economic and ecological environment. This study recommends further research into the lack of seasonal variation on the CEJ in this region and the cause of the latitudinal storm time variation.

TABLE OF CONTENTS

ABBREVIATIONS AND ACRONYMS

H	Horizontal intensity of the geomagnetic field
EEJ	Equatorial Electrojet
EMT	East of Prime Meridian
CEJ	Counter Electrojet
IQDs	International quiet days
IDDs	International disturbed days
Sq	Solar quiet
H_d	The geomagnetic field of the disturbed day
S_D	Disturbance daily variation
SC	Storm Commencement
SqH	Solar quiet variation in the horizontal intensity
Sq(H)	Solar quiet mean variation in the horizontal intensity
CME	Coronal mass ejection
CIR	Co-rotating interaction region
SEPs	Solar energetic particles
GIC	Geomagnetically induced currents
GMT	Greenwich Mean Time
LT	Local time
Dst	Disturbance storm time
IEEY	International Equatorial Electrojet Year
$E_{d—d}$	Solar wind electric field
IMF	Interplanetary Magnetic Field

LIST OF TABLES

LIST OF FIGURES

CHAPTER ONE

INTRODUCTION

1.1 The Study Background

The magnetic field of the Earth is internally produced predominantly by the electric currents flowing in the fluid outer core of the Earth, followed by the induction of magnetized rocks in the lithosphere and externally from the current systems in the ionosphere. The ionosphere is the layer of the Earth's upper atmosphere where ions and electrons are found in numbers that are enough to affect the radio wave propagation. Geographically, the ionosphere is stratified into three broad regions of geomagnetic latitudes. These include; equatorial or low latitude regions, mid-latitude regions and the polar or high latitude regions (Silva, Yamaguti, Kuga, & Celestino, 2012). Figure 1.1 illustrates these regions.

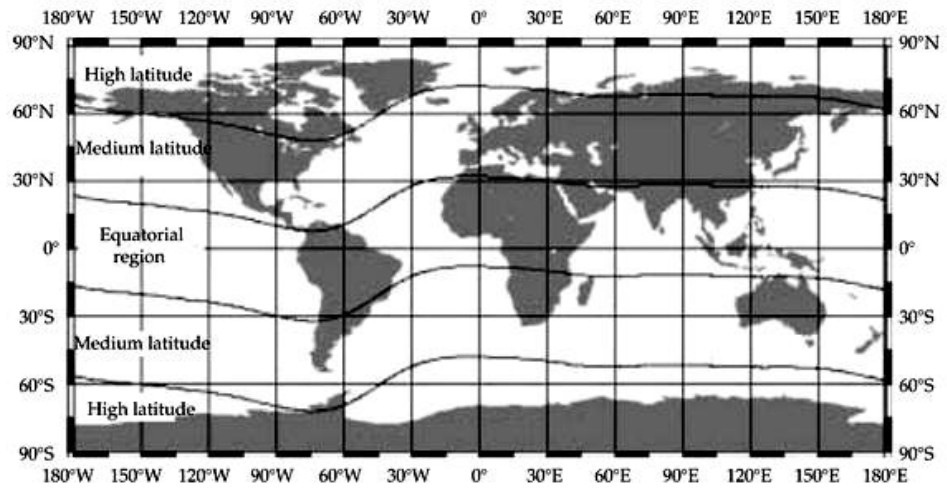

Figure 1.1: Geographical stratification of the ionosphere.

The equatorial regions range from about $+30^0$ to -30^0 of the geomagnetic latitude. This region is identified by the high magnitudes of electron content and the electron density which is distributed spatially in large gradients. In the current study, Addis Ababa -Ethiopia, Adigrat-Ethiopia, Yaoundé -Cameroon and Mbour- Senegal, all of which lie within the African

equatorial region, were selected as the stations for study. The field vector **B** of the Earth's magnetic field is obtained from the orthogonal components X, Y and Z which are the Northerly intensity, Easterly intensity and vertical intensity respectively. Z is positive downwards; F, H, I and D are the total intensity, horizontal intensity, inclination or dip (the angle between the horizontal plane and the field vector measured positive downwards) and the declination or magnetic variation respectively. D is the horizontal angle between the true North and the field vector, measured positive Eastwards. These elements of the Earth's magnetic field vector are illustrated in Figure 1.2.

(National Oceanic and Atmospheric Administration., 2020)

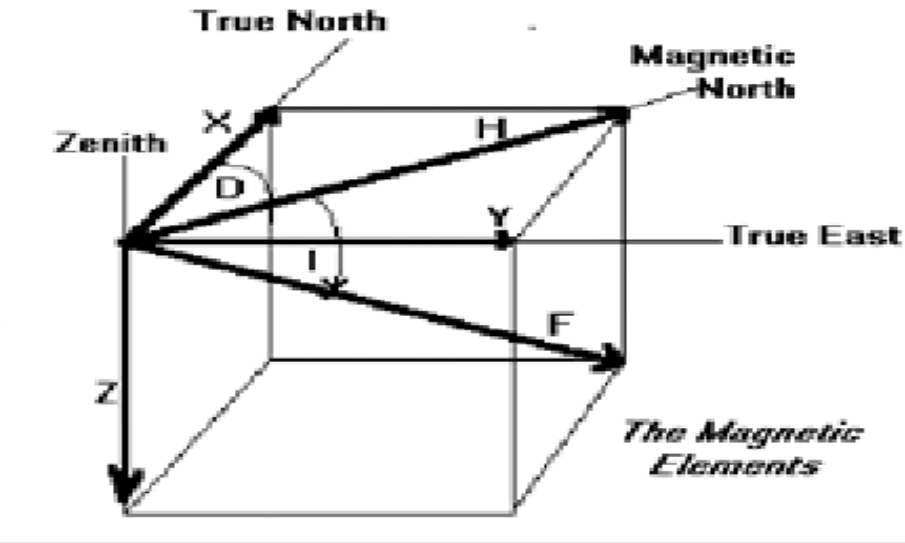

Figure 1.2: Geomagnetic Field Components.

The declination D, dip I and the total intensity F can be calculated from the orthogonal components using the following equations:

$$D = arctan\frac{Y}{X} \quad (1.1)$$

$$I = arctan\frac{Z}{H} \quad (1.2)$$

$$F = \sqrt{H^2 + Z^2} \quad (1.3)$$

where H is given by;

$$H = \sqrt{X^2 + Y^2} \quad (1.4)$$

The geomagnetic field has both regular variations due to the Earth's rotation about its axis within a basic period of 24 hours, known as solar quiet, and an irregular variation set up by a strong Southward interplanetary magnetic field (IMF) of 10nT to 15nT interacting with the Northward geomagnetic field lasting for a period between several hours to several days, called magnetic storm. The regular variations are seasonal and solar cycle dependent. They also rely on the local time and geomagnetic latitude (Shinbori, Koyamana, Nose, Hori, Otsuka, & Yatagai, 2014). They are produced by upper atmospheric electrical currents found at altitudes which range from 100km- 130km exceeding the Earth's surface because at these altitudes, the sun's ultraviolet (UV) and X-ray radiations noticeably ionize the atmosphere. The winds in the atmosphere and the tidal oscillations also force the ion section of this region of the atmosphere to move across the magnetic field lines in proportion to the electrons. The electrons however move very slowly and perpendicularly to both the field and the neutral wind thus producing an electric current (Baumjohann & Treumann, 1960). From Ohm's law; the conductivity of the ionosphere is given by;

$$\boldsymbol{J} = \boldsymbol{\sigma}.\boldsymbol{E} \qquad \textbf{(}1.5\textbf{)}$$

where; σ is the conductivity, **E** denotes electric field while **J** denotes current density.

To find a relationship of the conductivity, σ, electric field, **E** and the neutral wind velocity, v_n term is added for electric field giving Ohm's law equation as:

$$\boldsymbol{J} = \sigma.(\boldsymbol{E} + \mathbf{V}_\mathrm{n} \times \mathbf{B}) \qquad (1.6)$$

A geomagnetic storm or solar storm is a short term interference of the earth's magnetosphere which is brought about by a solar wind shock wave. An interaction of the Earth's magnetic field with the sun's magnetic fields that envelop it can also result into a storm. The disturbance that drives the storm may be caused by a Coronal Mass Ejection (CME) or by a Co-rotating Interaction Region (CIR) which is solar wind of very high speed ranging from a minimum of 500km/s to a maximum of 800km/s. The prevalence of geomagnetic storms is dependent on the sunspot cycle, occurring more frequently when the solar activity is maximum and less frequently when solar activity is minimum. The geomagnetic storm is a magnetically disturbed period lasting from a number of hours to several days, identified by a reduction of the Disturbance storm time (Dst) index (Chapman & Bartels, 1940). This present study intends to analyze selected storms in the African equatorial region and compare their effects on magnetic for the various stations under study.

Geomagnetic field variations may be temporal, spatial or longitudinal and secular or transient. Some of the geomagnetic field variations which are of much significance to space weather observations at equatorial latitudes are the solar quiet (Sq) variation and the storm- time variation. Also of much interest is the Equatorial Electrojet current (EEJ), flowing on the dip equator as an eastward current that is enhanced or intensified in the ionosphere's E-region between heights of 100km and 120km (Rabiu, Nagarajan, Okeke, & Ayiribi, 2007).

The EEJ is a confined band of enhanced electric current in the dayside ionospheric E-region within $+3^{o}$ to -3^{0} of the dip equator. It is shown pictorially as an enhancement of the solar quiet variation on the Horizontal component of the earth's magnetic field (Adimula & Akpaneno, 2015). The dynamics of the equatorial ionosphere varies from one sector to another and in Africa

the dynamics vary along the magnetic equator across the continent from west to east (Rabiu, Yumoto, Falayi, Bello, & MAGDAS/CPNGroup, 2011). This electrodynamic longitudinal variation is caused by longitudinally varying magnetic field of the Earth which modulates the neutral winds in the thermosphere together with the ionosphere's plasma density (Zhang, Wang, Wang, Dang, Liu, & Wu, 2018). There is need to further investigate this disparity in the African equatorial region in the inclining phase of solar cyle 24 to establish the physical processes that contribute to this variation for various seasons under quiet and disturbed conditions.

The ionosphere which is the atmospheric region ranging from above 60km to 1000km altitude is known for large ion densities which are sufficient to affect radio wave propagation. The current system in the ionosphere is attributed to a dynamo action of the horizontal wind system and its electrical conductivity as a result of the electrons and ions found in the ionosphere. The ionospheric current is more concentrated at the dip equator due to the accelerated value of electrical conductivity of the upper atmosphere at the region which arises from an inhibition of hall current which arises since the geomagnetic field is horizontally structured and the ionosphere is horizontally stratified (Rabiu, Nagarajan, Okeke, & Ayiribi, 2007). It has therefore continued to attract research interest due to its increasing application in radio-communication. The current study seeks to find the effect of these currents particularly the Equatorial Electrojet in the African equatorial region to establish its annual and seasonal trends in order to plan for space weather events like radio blackouts, Solar radiation storms and Geomagnetic storms.

The geomagnetic field activity is measured using magnetic activity indices. These magnetic activity indices are mapped out to show the variations in the geomagnetic field established by the irregular current systems. They include but not limited to: Planetary K (Kp) index used in the study of ionosphere and magnetosphere to measure the Earth's magnetic activity globally. Its

related indices are ap, Ap, and Cp; Disturbance storm time index (Dst), a measure of the intensity of the Equatorial Electrojet which is symmetrical worldwide and the Aural Electrojet, (AE) index, which gives a worldwide measure of quantity of the magnetic activity of auroral zone. This study made use of the Kp and the Dst indices. Kp is used because it can broadly characterize the various levels of Earth's magnetic activity worldwide in the range of 0 to 9 (Mayaud, 1980). Kp relates to the geomagnetic size measured in the most disturbed horizontal component of the Earth's magnetic field at a group of given stations quasi-logarithmically. The Dst index makes use of the 1 hour time resolution of the geomagnetic field data and depends linearly on the perturbation amplitude. This therefore, makes it suitable for describing magnetic activity in a short time scale during storms. In order to derive the Dst values, horizontal geomagnetic component is taken at four observatories which lie uniformly along a longitude and the hourly values are used (Mayaud, 1980).

A solar cycle is an 11 year period in which sunspot numbers and size fluctuate and the solar filaments are repeated. During the solar cycle, the sun's magnetic field reverses as its stormy behavior generates to a maximum. The next cycle is started when the sun has settled back to a minimum activity. Solar cycle 24 is the latest to be completed. It is the 24^{th} since the occurrence of the Maunder Minimum (1645-1715) (Owens, et al., 2017), when consistent recording of sunspot activity of the sun was started. Cycle 24 commenced in December 2008 and showed an inclining or ascending solar activity through 2014 to 2015 after which it started declining as indicated by the solar cycle sunspot number progression graph in Figure 1.3 up to the year 2021. The ascending phase of a solar cycle is a stage identified by a growing number of sunspots, an increase in their groupings and regions covered (Rawat, Echer, & Gonzalez, 2018). This study focused on this phase for the solar cycle 24.

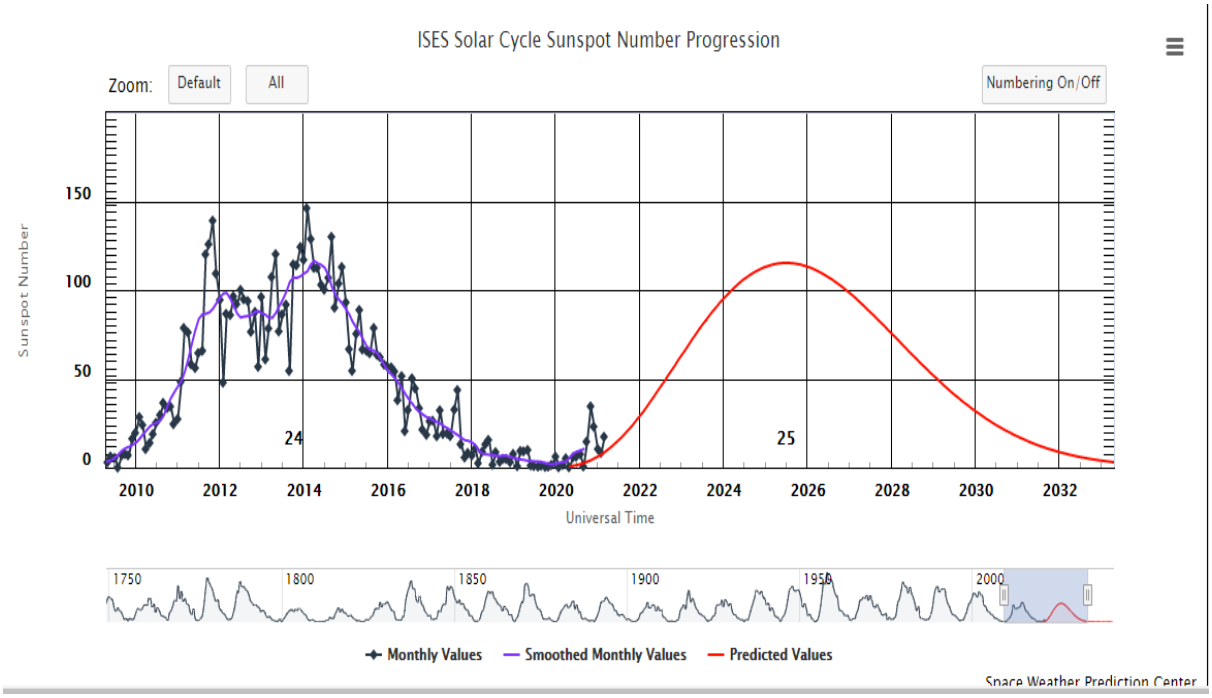

Figure1.3: Solar cycle 24 sunspot number progression by ISES (NOAA, 2021).

The annual and seasonal variability of the solar quiet (Sq) and storm time fluctuations as well as the EEJ strength had been studied in the recent past by a number of researchers; (Abbas, Joshua, Bonde, Adimula, Rabiu, & Bello, 2012), (Haines & Owens, 2019), (Rabiu, Mamukuyomi, & Joshua, 2007), (Omondi, Baki, & Ndinya, 2016) and (Babayev & Allahverdiyeva, 2007). However, the following have not been studied; the solar quiet seasonal and annual variations of the Earth's magnetic field in the African equatorial sectors; the EEJ strength seasonal and annual variations in the Equatorial region of Africa, storm or disturbance time variations in the African equatorial regions using the stations in this study for the inclining phase of solar cycle 24. For this reason, the present work bridges the following knowledge gaps; the solar quiet seasonal and annual variations of the geomagnetic field for Adigrat, Addis Ababa, Younde and Mbour stations during the inclining phase of the solar cyle 24; the variation of the EEJ strength at Addis Ababa and Mbour and making a comparison on this variation

between the two stations and the storm time variations in Addis Ababa, Adigrat, Younde and Mbour stations comparing these storm time variations for these African equatorial regions.

1.2: Problem Statement

There is knowledge gap on geomagnetic field variations including seasonal and annual variations, storm time variations and the Estimation of Equatorial Electrojet Strength in the African Equatorial region. Though some research has been carried out in this region, there is still no sufficient information to characterize the Earth's magnetic field in the African Equatorial region during the ascending period of the solar cycle 24. Based on the aforementioned knowledge gaps, the problem of this study was the little information on Geomagnetic field variations in the African equatorial region during the ascending phase of solar cycle 24 from the year 2009-2014 with a view to establish its solar quiet and storm time variations in Addis Ababa, Adigrat, Mbour and Yaoundé stations and to estimate the EEJ strength in Mbour and Addis Ababa for the period 2009 to 2014 that should help to identify the specific and unique trends within this region, that may be useful for industries and space agencies in the region for purposes of planning and preparations for space weather eventualities.

1.3: Objectives of the study

1.3.1: Main objective

The main objective of this work was to study the Geomagnetic Field Variations at African equatorial Region during the Ascending phase of Solar Cycle 24 from the year 2009-2014

1.3.2: Specific objectives

The specific objectives were:

i) To determine the solar quiet seasonal and annual variations of geomagnetic field at Addis Ababa- Ethiopia, Adigrat-Ethiopia, Yaoundé-Cameroon and Mbour- Senegal during the Ascending phase of solar cycle 24 from the year 2009 -2014.

ii) To estimate the EEJ strength at Addis Ababa and Mbour for the period from 2009-2014.

iii) To determine the storm time variations of the Earth's magnetic field at Addis Ababa – Ethiopia, Adigrat- Ethiopia, Yaoundé-Cameroon and Mbour- Senegal for selected storms for the ascending phase of the solar cycle 24.

1.4 Hypotheses

i) There are seasonal and annual or semi-annual variations of the geomagnetic field in the African equatorial regions in the inclining phase of solar cycle 24.

ii) The EEJ depicts seasonal and annual variation.

iii) The geomagnetic storm effects do not depend upon the geomagnetic latitude of a station.

1.5 Justification of the Study

From the previous research work presented in this thesis and to the best of my knowledge, there is no research that has been carried out within the African equatorial region which sought to determine the geomagnetic field variations simultaneously for the stations in this study and covering the quiet time, storm time and the determination of EEJ during the ascending stage of solar cycle 24, despite the need for these information in this region. The present study takes advantage of the fact that the geomagnetic equator passes through Africa and the selected stations which fall within the dip equatorial region have the ground based magnetometers

installed. The region is selected for study since it has been observed that the Earth's magnetic field is almost horizontal here, hence it is more liable to form most important phenomena arising from electromagnetic interactions like EEJ and CEJ.

1.6: Rationale of the study

Information on geomagnetic field variations in the African equatorial region is still not well developed although such information would be very useful to stakeholders in many industries such as aviation, mining and even electric power distribution companies. This study provides information useful for modeling of geomagnetic field variations over equatorial African region as it is a critical component of space weather monitoring.

1.7: Significance of this study

This study will enable government space agencies to make necessary arrangement to curb the effects of such phenomena as Solar radiation storms, Geomagnetically Induced Currents (GICs) which have presented a major threat to power grids and the disturbances within the ionosphere that may affect radio communication, radar scintillations and disruption of magnetic compass navigation

1.8: Assumptions of the study

When selecting quiet days, that is $Kp \leq 2$, we can completely eliminate the effect of changes in activity of the geomagnetic field.

1.9: Limitations of the study

The study met a challenge of data gaps from the AMBER stations due to failure of the magnetometers to capture and save data in some years. The results for Adigrat station for the years 2009 and 2014 were therefore not included though there is a possibility that these could

have marked years of minimum solar activity and maximum solar activity respectively which are significant in determining peak magnitudes of Sq. However, the periods with missing data were exempted from the analysis. The available data was still sufficient to achieve the objectives of the study. Table 1.1 shows the available data as a percentage for each station for each year of study.

Table 1.1 Percentage available data per station per year

	STATION CODE			
YEAR OF STUDY	AAE	MBO	ETHI	CMRN
2009	100%	100%	0	79.88%
2010	100%	100%	60%	100%
2011	100%	100%	71%	94%
2012	100%	100%	89%	93%
2013	100%	100%	88%	88%
2014	100%	100%	0	90%

CHAPTER TWO

LITERATURE REVIEW

2.1 Introduction

This chapter gives a framework for establishing the importance of this study and the need for further studies by highlighting the knowledge gap, critiquing other literature with regards to their findings, methodology, analysis and evaluation. It has been broken down into subtopics in line with the objectives of this study as follows; previous studies on solar quiet variation of the Earth's magnetic field, previous studies on Equatorial Electrojet and previous studies on disturbance time variation of the Earth's magnetic (Geomagnetic) field.

2.2 Previous Studies on Solar Quiet Variations of the Geomagnetic Field

A study of how the magnitude of Sq varies at a constant hour from day to day, (Okeke, Onwumechili, & Rabiu, 1998) used data from nine stations between the dip equator and latitude 22^0 North. The results showed that the magnitude and sign of the variability portrayed a random change which reasonably reduced the mean to zero. This variability occurred throughout the day. Its D, H and I amplitudes have equal diurnal variation, whose peak was seen at local noon, with a June solstice peaked seasonal variation which was relatively weak. The results suggested that the conductivity of the ionosphere is majorly what controls the amplitude while the phase and how random the hourly day to day variability amplitudes of Sq were controlled by the electric field and in turn the winds (Okeke, Onwumechili, & Rabiu, 1998). Their work looked at amplitude of Sq per hour with regards to its day to day variability, while the present study looks at the seasonal variation and annual variation of Sq using H component.

In another study on the variation of the Earth's magnetic field for a station located within the dip equatorial region using data from a station in Sri Lanka, Peredinia, (Rastogi, Kitamura, & Kitamura, 2004) realized that the variation of H on a daily basis showed maximum peak near midday. The variation of Z per day seemed to be the gradient of the curve of variation of H per day with time with its maximum amplitude occurring at around 09.00LT (75^0 EMT) when H field was fast increasing, and not at noon when geomagnetic horizontal field ΔH was at the peak. The variation of H during a storm was similar to the Dst index variation. The present study, however, seeks to establish these variations in the African equatorial regions during the ascending period of solar cycle 24.

Geomagnetic field variations were studied in West Africa at the latitudes within the dip equator using data from the participation of France in the 1993 African IEEY (Obiekezie, 2012). An examination of quiet conditions on the H, D and Z components of the geomagnetic field indicated that D element had more variability than H and Z. Also noticed was the existence of night time variation in this region which was attributed to magnetospheric currents such as the ring current. There is need to study the consistency of these trends in the recent solar cycles hence this study seeks to study the geomagnetic field variations in the solar cycle 24 during its inclining phase.

Sq (H), the mean of SqH, varies in amplitude according to seasons of the year and the variation is transient. This is according to the result of the study conducted for the year 1996 on the variation of Sq in different seasons across various latitudes and longitudes. The data was obtained from 64 different geomagnetic stations across the globe (Owolabi, Rabiu, Olayanju, & Bolaji, 2014). The present study not only focuses on the seasons and the SqH, but also studies

the annual SqH variation and the disturbance time variation in the geomagnetic H-component across the African equatorial regions.

While comparing solar cycle 24 with the past solar cycles with an aim to establish the reality of solar activity behavior during the phase of solar cycle 24, it was shown that at least for the last century, the solar minimum that led to the transition from solar cycle 23 to 24 from the year 2007 to 2009 has been longest. According to that study it was also shown that the Dalton minimum period had a solar activity that resembled the progress of solar cycle 24. The study also confirmed that there is an influence on the space weather and the external conditions of the earth's atmosphere as a result of the quite weak activity of the 24^{th} solar cycle (Narang, Gupta, & Gaur, 2016).

A study of the variation of the geomagnetic field at the quiet time based at the East African equatorial region showed that local time and activity of the sun affect the Sq (H), the mean of Sq. The highest amplitudes occur between 1100LT and 1200LT and it increases as the solar activity increases. This dependence on local time is attributed to changes in solar heating and the varying rates of ionization (Omondi, Baki, & Ndinya, 2016).

Data from six MAGDAS magnetic observatories was employed to characterize the horizontal component of earth's magnetic field investigating its seasonal, annual and hourly variations in some stations along the 210^0 magnetic meridian from the year 2007 to 2009. The results indicated that the highest values of Sq are realized during equinoxes at around 1300LT. The highest annual magnitude recorded was 70.96nT in 2009 while the lowest value was 27.25nT in the same year (Idowu & Adimula, 2020). The present study seeks to investigate the seasonal and

annual variations of the geomagnetic field in selected stations at the equatorial region of Africa starting the year 2009 to 2014.

Inter-hemispheric field aligned currents (IHFACs) seasonal variation was studied for the solar cycle 23 and 24. This was done by analyzing geomagnetic field data within the equatorial region using time series. The results showed that the night side IHFACs flowed in a common direction as the noon side in June solstice as in December solstice. The night sector was also observed to depend on the solar cycle (Ranasinghe, Fujimoto, & Jayarante, 2021).

A study to estimate the latitudinal positions of the Sq focus of the northern and southern Sq loops in the Indian sector by (Archana & Arora, 2022) was conducted for the solar cycle 24 using the X and Y components data from 13 sites. The results showed that the Sq focus in the northern hemisphere exhibits annual variation with maximum equatorward movement at the summer solstice and maximum poleward movement at the winter solstice whereas the Sq focus in the southern hemisphere exhibits a semiannual variation with maximum Equatorward movement at the spring and autumn equinoxes and maximum poleward movement at the summer solstice (in the northern hemisphere). The results also showed that the seasonal variations in EEJ show a weak relationship with Sq focus movement. They attributed the observations to the northern Sq focus being closer to the equator in September than in March.

The present study seeks to establish these variations in the African equatorial region and compare the findings at different stations in the region during the ascending phase of solar cycle 24 as well as to establish the storm time variation during this period for selected days.

2.3 Previous studies on the Equatorial Electrojet

The study of low latitude geomagnetic day to day variability hourly magnitudes has shown a contrast in phases of the intensities of EEJ current and the global part of Sq. They sometimes appear in antiphase, but the changes are generally independent of each other. In case the D component of the magnetic field is included then, in addition to the East to West component of the EEJ current system there is also a North–South element (Okeke, Onwumechili, & Rabiu, 1998).

The variations of the geomagnetic field was investigated at low latitudes within the equatorial zone using the Japanese new designed Ocean Hemisphere Network Project to carry out long term observations on the pacific remote places. The H, D and$Z$ components of the geomagnetic field were analyzed and the results showed that the magnitude of dH depicted diurnal variation whose peak was observed during the day around 1200LT in the three EEJ regions that were investigated. According to this research, the H component showed a diurnal variation with the enhancement of Sq in these regions because of the enhanced equatorial dynamo action. On the other hand, the D component diurnal variation indicated that the EEJ current system comprised of an East-West component as well as a North –South component (Okeke & Hamano, 2000).

(Haile, 2003) studied the strength of the Equatorial Electrojet during various periods of solar activity in the African equatorial sector. He observed that the H component daily variation at Addis Ababa showed a local noon peak of ΔH. This shows the stations strength of the eastward electric field at the equator. It was noted that during the months of local winter (November, December, January and February) the peak occurred earlier than in the months of local summer (May, June, July and August). This study seeks to extend this analysis in order to find the time delay for different years and compare this trend for Addis Ababa and Mbour stations.

A comparison of the EEJ current density estimated from high quality scalar magnetic field measurements of the CHAMP satellite with the magnetic horizontal intensity variations at six equatorial ground based observatory pairs distributed across the globe was done. Signals were analyzed for correlation using data from 2000-2002 solar maximum year observations. The analyses showed that the longitudinal correlation length was short, a fact that was linked to the instabilities in the local plasma within the cowling strip. From this analysis, a suggestion was made on the need to dedicate an array of magnetometers to help cope with the various features of intercoupling of EEJ and Sq appropriately (Manoj, Luhr, Maus, & N.Nagarajan, 2006). This study makes use of the AMBER and INTERMAGNET array of magnetometers within the African equatorial region to establish this link between EEJ and Sq within the region.

(Rastogi & Trivedi, 2009) studied the discordance in the Equatorial Electrojet in the North- East Brazil region by analyzing the data from X, Y and Z components of the geomagnetic field from an array of vector magnetometers in 26 stations from November 1990 to March 1991. The combined ΔY and ΔX showed the flow of Equatorial Electrojet currents to be directed along 25° North-East at the edge of the Equatorial Electrojet belt. They reported that the EEJ current strength to the North of the belt was greater than that to the south of the belt and suggested that these irregularities were due to the anomalous distribution of the average magnetic field at the region. The current study however, analyses the H component of the Earth's magnetic field to compare the EEJ current strength at Addis Ababa and Mbour stations in the African equatorial regions.

(Adebesin & Yumoto, 2013) used data fron an equatorial stations in describing the characteristics of the F_2 layer and the strength of Electrojet. They recorded that the June solstice peak value of the seasonal daytime strength of EEJ current was ranging between 27-35nT and occurred at around 1400LT. The March and September equinoxes had peaks with magnitudes ranging from 30-40nT and 35-40nT at 1200LT and 1500LT respectively. These differences in EEJ strengths were attributed to the collective effect of the electric field and the maximum electron density.

(Adimula & Akpaneno, 2015) studied Horizontal component variability of the Earth's magnetic field from ten MAGDAS magnetometers along the magnetic equator. They studied the variation trend of the Sq and disturbed variation. The H variation with Sq (H) enhancement in all ten stations which peak around local noon with a steady similar pattern of variation in all EEJ was linked to the intensified dynamo action in the regions. The changing Sq (H) was ranging from 20nT to 170nT with peaks around 1200- 1300hours LT. They also observed that the magnitude of variation on disturbed days were generally higher due to the disturbances within the ionosphere emanating from the sources from outside it external like effects of space weather and storms. Their results confirmed the presence of CEJ occurring in the morning and evening hours with maximum amplitude of -25nT recorded during pre-sunset as well as a longitudinal variability in the EEJ. They recorded a pronounced equinoctials maximum which was attributed to the enhanced electron density at equinox.

The study of solar Cycle 24 and its expected features by (Shailraj Narang, 2016) indicated that the cycle seemed to show a Dalton type of progression. The solar activity was a minimum cycle. In this study, Narang also showed quite a weak solar activity in cycle 24 and this influences the space- weather conditions.

In the East African sector, a correlation analysis was carried out between the EEJ and the equatorial ionization anomaly (EIA) occurrence. This was done using statistical analysis by differential technique to determine the EEJ for quiet geomagnetic conditions and to derive total electron content (TEC) by finding the TEC ratio across the trough as the CT: TEC ratio (current transformer to total electron content ratio), in order to get the EIA strength for the region. The trough was found to lie rather to the south of the dip equator possibly as a result of the slight shift of the EEJ centre to the south of dip equator at the East African region, The study highlighted a positive correlation between the EEJ and EIA Strengths during the day, with the strongest positive correlation witnessed from 13:00 to 15:00LT (Mungufeni, Habarulema, Orue, & Jurua, 2018).

(Tuo, Doumbia, Coisson, & etal, 2020) examined the seasonal variation while studying the variation peaks. The longitudinal EEJ profiles was studied using the satelite magnetic measurements of full CHAMP in the period 2001 to 2010.A longitudinal pattern of wave four was observed on EEJ averagely. A detailed analysis of the Monthly averages when analysed into datails, gave two categories of longitudinal profiles; a main phase which had three maxima and a secondary phase with one maximum forming the EEJ wave four pattern of variation. This study however, did not investigate the annual aspects of EEJ longitudinal variation profiles.

An estimation method and the Fambitakoye simulation model were used concurrently to study the electrojet current in order to establish the correlation between the findings of the results from these two methods. The hourly magnetic field horizontal component Data from MAGDAS stations along the 210^0 magnetic meridian for the year 2007 were used to study the EEJ. The Fambitakoye model gave higher values than the estimation method even though the performance of the two methods was observed to be similar. The stations nearer to the dip equator showed

higher amplitudes of the EEJ current than stations away from the dip equator (Idowu, Adimula, & Adebesin, 2020).

2.4 Previous studies on Disturbance Time Variations of the Earth's magnetic Field

The longitudinal symmetric and asymmetric components of the D and H fields were derived from data obtained from the mid latitude stations in order to investigate the magnetospheric storm time currents. From the results of the symmetric D component, the morning side depicted a net downward field aligned currents while the evening through early morning side showed an upward field aligned currents for the period that the interplanetary magnetic field is directed to the south. At the commencement of the storm time ring current, the study identified an afternoon net downward current (Iyemori, 1990). The current study used the Horizontal element of the geomagnetic field data from ground based magnetometers to analyze selected storms in the equatorial regions of Africa for the purpose of investigating their trend and effect in this region.

In a study of the Earth's magnetic variations and the time derivatives of these variations during geomagnetic storms occurring at various intensity level, (Watermann & Gleisner, 2009) analyzed how the horizontal variations of the geomagnetic field, ΔH was statistically distributed with the time derivatives $^{\partial H}/_{\partial t}$ for a period of 3 years from the year 2003 to the year 2005. Their findings were that the magnitude distribution of ΔH and $^{\partial H}/_{\partial t}$ differ structurally based on geomagnetic latitudes and the level of the intensity of the storm.

(Mandrikova, Solovev, & Zalyaev, 2014) came up with a method to describe the geomagnetic field variations which was based on wavelets. They developed an algorithm to select the decomposition level of wavelets and adjustable set up of the neutral network. They carried out a collective Earth's magnetic field and cosmic rays examination for the times when the

geomagnetic storms were strongest. The perturbations were very strong during the times when there were anomalies in the variations in levels of cosmic rays.

(Watani, 2017) studied the magnetic storms during cycle 24 together with the solar origin of these storms. He concluded that considering the solar cycles from cycle 14 which occurred between 1902 and 1913 to date, solar cycle 24 is very weak and depicts very low geomagnetic activity. This very low geomagnetic activity was attributed to low electric field of the dayside solar wind which occurs at rate of E_{d-d}>5mV/m, the rate decreasing in recess from 2013-2014. He noticed that these geomagnetic storms were majorly contributed by the relatively slow CMEs.

.(Haines & Owens, 2019) while studying how the geomagnetic storm varies in time span with its intensity used the long running global geomagnetic disturbance index, aa, to analyze how connected is the intensity of the storm and its duration. They found a nonlinear relationship between the two and the duration was longer for the storms of very high intensity than for those of a shorter intensity.

A cross correlation analysis done on the IMF and solar wind effects on the geomagnetic H component during the storms on geomagnetic field, used data from four stations on low latitude with 145^0 to 215^0 longitudinal separation to investigate the relationship between the horizontal component and the density of solar wind and IMF for the strongest SSC and strongest moderate storms of cycle 23. The results showed a unique response of the magnetosphere to the various sources without it since a dawn to dusk variation was not observed in the profile. There was however, a superposition of the profiles of the cross correlation coefficients and the time gap (Chiaha, Ugonabo, & Okpala, 2019).

In a study of Geomagnetic storms related to the Disturbance Storm time indices (Dst), (Lin, 2021) established that Dst index varied in relation to the extremely small negative integer that indicated a large geomagnetic storm. The large sharpened variants of negative Dst indices could describe the detailed features of a geomagnetic storm.

In spite of the various studies conducted, as reviewed above, the dynamics of ionosphere depend on region, local time, geomagnetic latitudes and longitudes, solar cycle and even season of the year and geomagnetic activity. The African equatorial regions, during the ascending phase of the solar cycle 24 for the stations under this study, has not been investigated fully for the geomagnetic field variations during quiet and disturbed conditions. This study therefore aims at determining the geomagnetic field variation at African equatorial stations for the inclining period of solar cycle 24 to enhance further understanding of this cycle 24.

CHAPTER THREE

MATERIALS AND METHODS

3.1 Introduction

This chapter highlights detailed research procedure, study area, dataset, measurements of variables with the appropriate techniques employed for data analysis. Confounding variables have been identified and how they have been taken care of explained in this chapter. The chapter has been precisely presented to enable other researchers to replicate the study in case of such a need.

3.2 Materials (Data sources)

Magnetic field measurements from International Real-time Magnetic Observatory Network (INTERMAGNET) stations in Ethiopia, Addis Ababa and Mbour in Senegal and African Meridian B-field Education and Research (AMBER) arrays data at Yaoundé Cameroon and Adigrat Ethiopia for the duration from January 2009 to December the year 2014 were used. Table 3.1 shows the geographic as well as the geomagnetic coordinates for the various stations used in this study.

Table 3.1 Geomagnetic and Geographic Latitudes and Longitudes used

Name of Station	Station code	Geographic Latitude	Geographic Longitude	Geomagnetic Latitude	Geomagnetic Longitude
Addis Ababa	AAE	9.0^0N	38.8^0E	0.9^0N	110.5^0E
Adigrat	ETHI	14.3^0N	39.5^0E	5.80^0N	111.06^0E
Yaoundé	CMRN	3.87^0N	11.52^0E	5.30^0S	83.12^0E
Mbour	MBO	14.43^0N	16.97^0W	2.06^0N	58.24^0E

It must be noted that although Mbour is geographically west, it is Geomagnetically located East of the geomagnetic meridian.

These stations were paired for the estimation of EEJ strength using the two station method. The difference between H components at two stations; one within the dip equator and one located off-dip equator was established for the following pairs Addis Ababa and Adigrat on one side and Mbour and Yaoundé on the other side. The reason for this was to estimate the geomagnetic element EEJ indices.

Geomagnetic activity indices, planetary magnetic index, Kp and Disturbance storm time index, Dst, were used to identify the most quiet and highest disturbed days of every month for the whole period of study. The classification criterion for quiet time was Kp less or equal to 2 and Dst greater than -20nT starting 1st January, 2009 and ending 31st December, 2014, while the criterion for geomagnetic disturbances was Kp greater or equal to 2+ and Dst less or equal to -50nT(Yamazaki, Richmond, Liu, Pedatella, Maute, & Sassi, 2014)from the magnetic activity index list of Kp and Dst indices found at http://wdc.kugi.kyoto-u.ac.jp/cgi-bin/kp-cgi, a website of world data centre for geomagnetism located at Kyoto, Japan.

The locations of magnetometer stations that were employed for study are given in Figure 1.3 below.

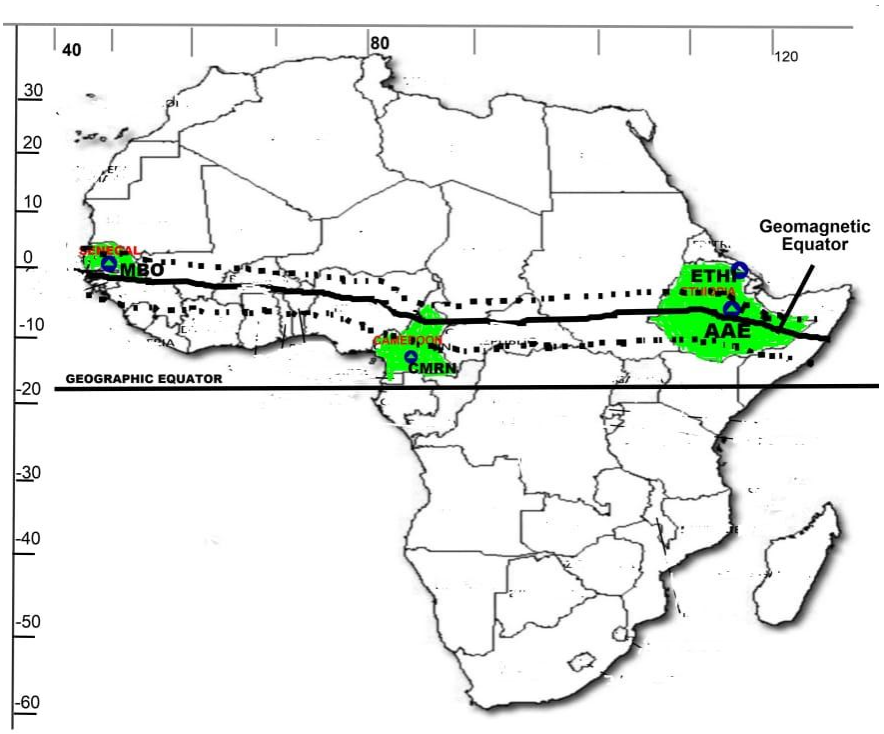

Figure 3.1: Geomagnetic location of the magnetometers network which have been used for this study.

3.3. Methods

3.3.1: Determination of Solar quiet seasonal variation of the Earth's magnetic field

The H- component for a single day from stations under study was calculated as per equation 1.4.

That is; H is given by: $H = \sqrt{X^2 + Y^2}$ (ref. equation 1.4)

Daily baseline for the geomagnetic field component, used in this study was:

$$H_0 = \frac{H_{23}+H_{24}+H_1+H_2}{4} \quad (3.1)$$

where H_1, H_2, H_{23} and H_{24} are the hourly values of H during the 4 hours flanking local midnight (Rabiu, Nagarajan, Okeke, & Ayiribi, 2007). Night time values are preferred because the ionospheric E-region which provides the dynamo current disappears at night and the magnetic

field around midnight is considered to be constant, constituting only the main field (Onwumecnihli, 1997). Hourly deviations of H component from midnight baseline, ΔH were calculated by getting the difference between the values of midnight baseline for a given day and the hourly values of that given day;

$$\Delta H = H_t - H_0 \tag{3.2}$$

where $t = 1\ to\ 24$ hour LT (Rabiu, Nagarajan, Okeke, & Ayiribi, 2007).

During quiet conditions, it is expected that the geomagnetic field should display a pattern of variation similar to periodic function in which, the magnitude at 00hr LT is the same as the magnitude at 24hr LT. Usually, it is not so and a non-cyclic variations correction needs to be done on the availed data (Rastogi, Kitamura, & Kitamura, 2004).

In this study, the hourly deviations were rectified for non-cyclic variations by linearly adjusting the daily hourly magnitudes of ΔH then considering the hourly departures ΔH at 01LT, 02LT,……., 24LT as V_1, V_2,……,V_{24} then taking the non-cyclic variation factor as:

$$\Delta_c = \frac{V_1 + V_{24}}{23} \tag{3.3}$$

The linearly modified values for the hours become:

$$V_1 + 0\Delta_c,\ V_2 + 1\Delta_c, V_3 + 2\Delta_c, \ldots\ldots\ldots V_{23} + 22\Delta_c, V_{24} + 23\Delta_C \tag{3.4}$$

$$S_t(V) = V_t + (t-1)\Delta_c \tag{3.5}$$

where t is the local time from 1 to 24 hours (Rabiu, Nagarajan, Okeke, & Ayiribi, 2007). The calculation of the H component and correction for non cyclic variations was carried out as per the scripts in appendices I and II. These corrected hourly departures on non-cyclic variation gave the solar variation in H for each day, Sq (H), an average of daily variations was established for

all the quiet days of individual months within the study period to get mean monthly variations in Sq. The approximation of seasonal variations was then done by finding the average of the monthly values for every season. The grouping of the months into seasons was done as: December solstice or D season covering the months of November, December January and February; March equinox or March E season covering March and April; June solstice or J season covering the months of May, June, July and August and September equinox or September E season which took care of September and October in accordance to the works of (Rabiu, Mamukuyomi, & Joshua, 2007).

The monthly averages of SqH variations across all years was obtained using MATLAB software to define the solar quiet annual variation of the H- field. Appendix III shows the script used for this analysis. The results for Sq seasonal variations are shown in Figure 4.1.1, Figure 4.1.2, Figure 4.1.3 and Figure 4.1.4 while results for annual variations are shown on Figure 4.1.6.

3.3.2 Estimation of seasonal and annual EEJ strength at Addis Ababa and Mbour

The strength of Equatorial Electrojet was estimated by taking the difference in the amplitudes of the SqH of the geomagnetic field at a station within the dip equator, whose dip latitude range is within $\pm 3^0$ and a station within the low latitude but off the dip equator within $\pm 6\text{-}9^0$ of almost equal longitude sector. This is because the station within the EEJ strip has Sq current enhanced with Equatorial Electrojet current while the one outside only has Sq current (Rabiu, Nagarajan, Okeke, & Ayiribi, 2007).

$$\boldsymbol{EEJ} = \boldsymbol{Sq}\ at\ the\ EEJ\ strip - \boldsymbol{Sq}\ outside\ the\ EEJ\ strip \tag{3.6}$$

The universal time presentation of the data was converted to local time convention for analysis. This was done according the relation:

$$LT = UT + [\frac{\Theta}{15}] \quad (3.7)$$

where Θ is the geographic longitude of the station being studied.

This is because during the 24 hour rotation of the Earth, it covers a longitudinal difference of one degree which gives a difference of 4 minutes in time.

The Lloyd seasons were used to group months in order to study the seasonal variation as explained in section 3.2.1; each season was approximated through finding the monthly average of the H hourly for all months making up a given season. Each year was approximated by finding monthly averages of H for the particular months making a year. The EEJ seasonal and annual variations were studied and plotted using the script in appendix IV. The results for annual variations of EEJ are shown in Figure 4.2.1 while the results for seasonal variations of EEJ strength are shown in Figure 4.2.3.

3.3.3 Determination of storm time variation of the Earth's magnetic Field.

A storm day was selected from the Kp and Dst index values listed by world data centre Kyoto. The selected days and their corresponding maximum Kp and highest negative Dst values are given in Table 3.2

Table 3.2 Selected storm days and their corresponding maximum Kp and highest negative Dst values

SELECTED STORM DAYS	MAXIMUM KP VALUE	HIGHEST VALUES OF DST
2012, July16th	4+	-113nT
2011, July, 5th	2+	-59nT

The storm time daily variation S_d was derived by subtracting the baseline of the quietest day for a particular month from H_d, the geomagnetic field of the disturbed day for each of the disturbed days. This was done for all the months according to (Maeda, 1968). That is;

$$\boldsymbol{S_d = H_d - H_0}\text{: t=1,2,……24} \tag{3.8}$$

where S_d is the disturbance daily variation;H_d is the geomagnetic field intensity of a disturbed day and H_O is the quietest day baseline. The obtained disturbance daily variation was used to calculate the pertubation of the storm as;

$$S_D = S_d - S_q \tag{3.9}$$

where S_D is the perturbation of the storm; S_d represents the disturbance daily variation and S_q stands for the solar quiet variation.

The storm time perturbation was calculated and plotted using the script in appendix V and the findings are displayed in Figure 4.3.1 and Figure 4.3.2.

CHAPTER FOUR

RESULTS AND DISCUSSIONS

4.1 Introduction

In this chapter, statistical summary of the results of this study has been done, pointing out whether the findings herein support or contradict other studies and giving possible reasons for the outcomes. The chapter has been divided into three subtopics namely; Solar quiet seasonal and annual geomagnetic field variation, Results and discussions on EEJ strength for Addis Ababa and Mbour stations and Results and discussions on Earth's magnetic (geomagnetic) field storm time variations .

4.2 Solar Quiet Seasonal and Annual variations of geomagnetic field

The Figure 4.1.1, Figure 4.1.2, Figure 4.1.3 and Figure 4.1.4 illustrate seasonal variations in SqH for the four stations; AAE, CMRN ETHI and MBO respectively.

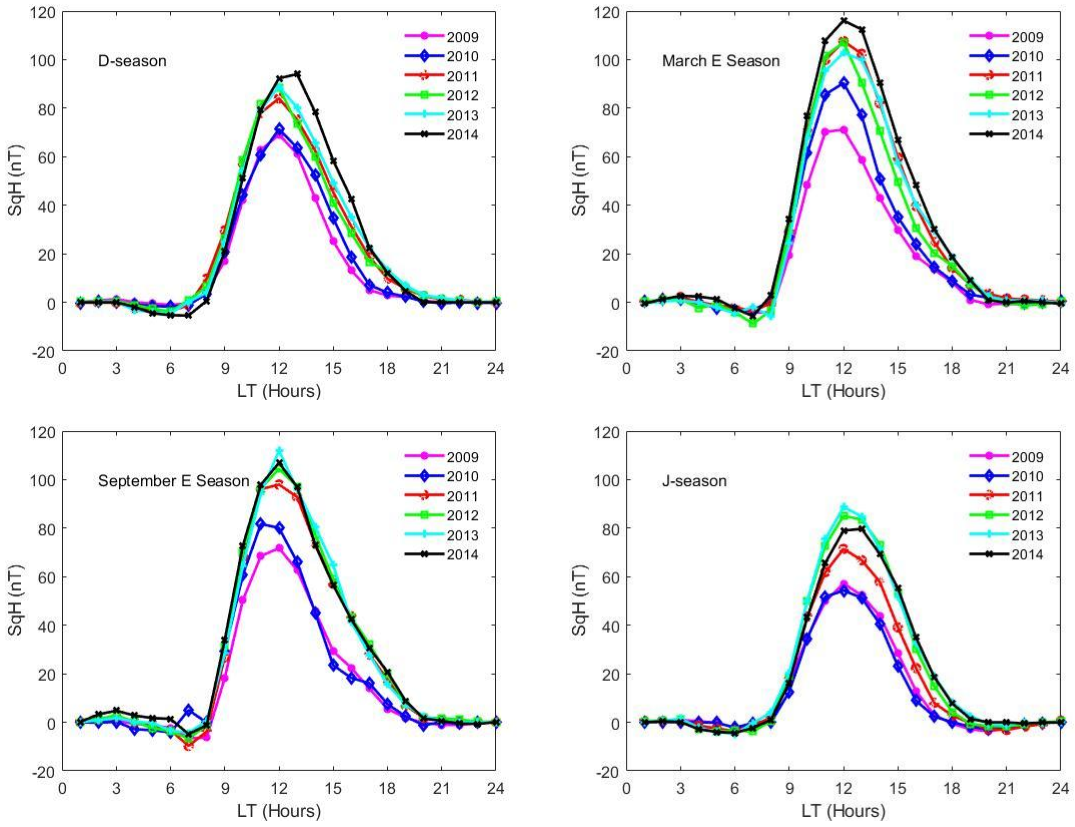

Figure 4.1.1: Seasonal variation of SqH at Addis Ababa, Ethiopia from 2009-2014.

The peak at Addis Ababa station occurs at local noon for all the seasons. The E- seasons both recorded the highest maximums in 2012 of around 110nT with peak at local noon. The minimum

The peak at Addis Ababa station occurs at local noon for all the seasons. The E-seasons recorded the highest maximums in 2012 of around 110nT with peaks at local noon. The minimum peaks for E-seasons were in 2010 of 90nT. Low peaks were recorded during the J season and D season and the lowest amplitude occurred in 2010 during the J season of 50nT. The magnitudes during the day were greater than those at night for all the seasons as a result of higher rates of photo ionization during the day as compared to low recombination rates at night.

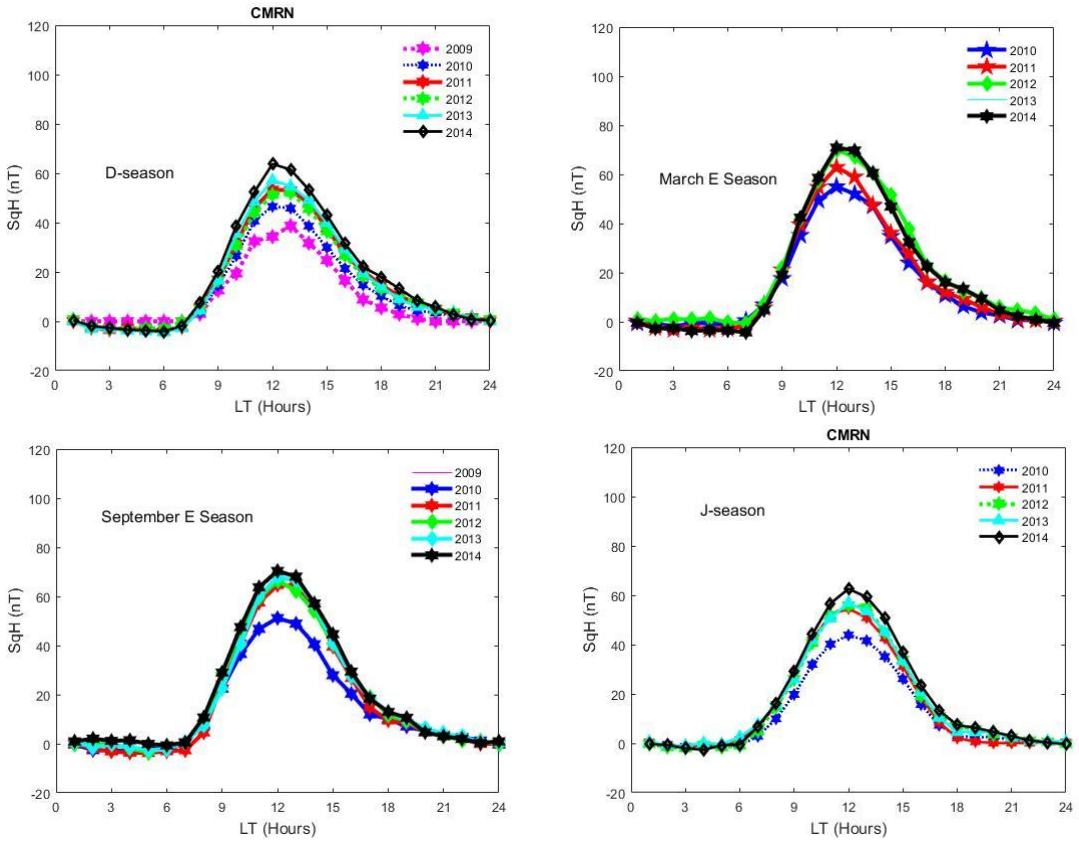

Figure 4.1.2: Seasonal variations of SqH at Yaoundé, Cameroon from 2009 to 2014.

The peaks occurred at local noon for all the seasons. The minimum peak was recorded in the year 2010 during the J season of about 40nT. The E-seasons recorded higher values of SqH than J and D seasons. The daytime magnitudes were higher than night time magnitudes in each of the seasons in the entire study period. This is attributed to the high ionization rates during the day as compared to during the night.

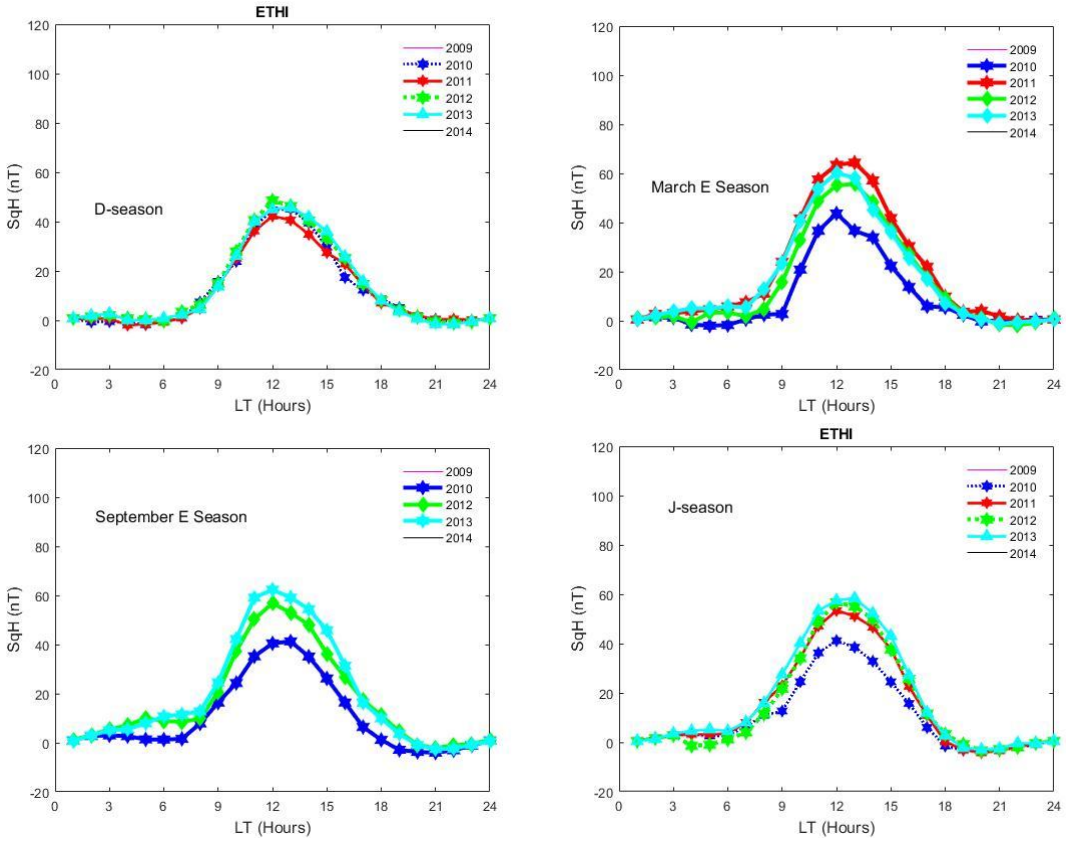

Figure 4.1.3: Seasonal variations of SqH at Adigrat, Ethiopia from 2009 to 2014.

electron density which increases the electrical conductivity as a result of the overhead position of Adigrat station showed the highest value of SqH of about 65nT in the year 2012 during the March Equinox. The E-seasons recorded generally higher values than J and D seasons. This is attributed to an enhancement in density of electrons at the equatorial region. The enhanced electron density increases the electrical conductivity during the equinoxial overhead sun. The

dynamics of the corresponding electric field also contribute (Idowu & Adimula, 2020). The Sq seasonal variation peaked slightly before noon during March Equinox but peaked at local noon in the other seasons. This is linked to the increased equatorial electron density that leads to an increase in the electrical conductivity as a result of the overhead position of the sun at the equinox. The minimum for this station occurred in 2010 during the J season. Adigrat also recorded higher daytime magnitudes of Sq as compared to the night time magnitudes. This is attributed to the high rates of ionization during the day than at night.

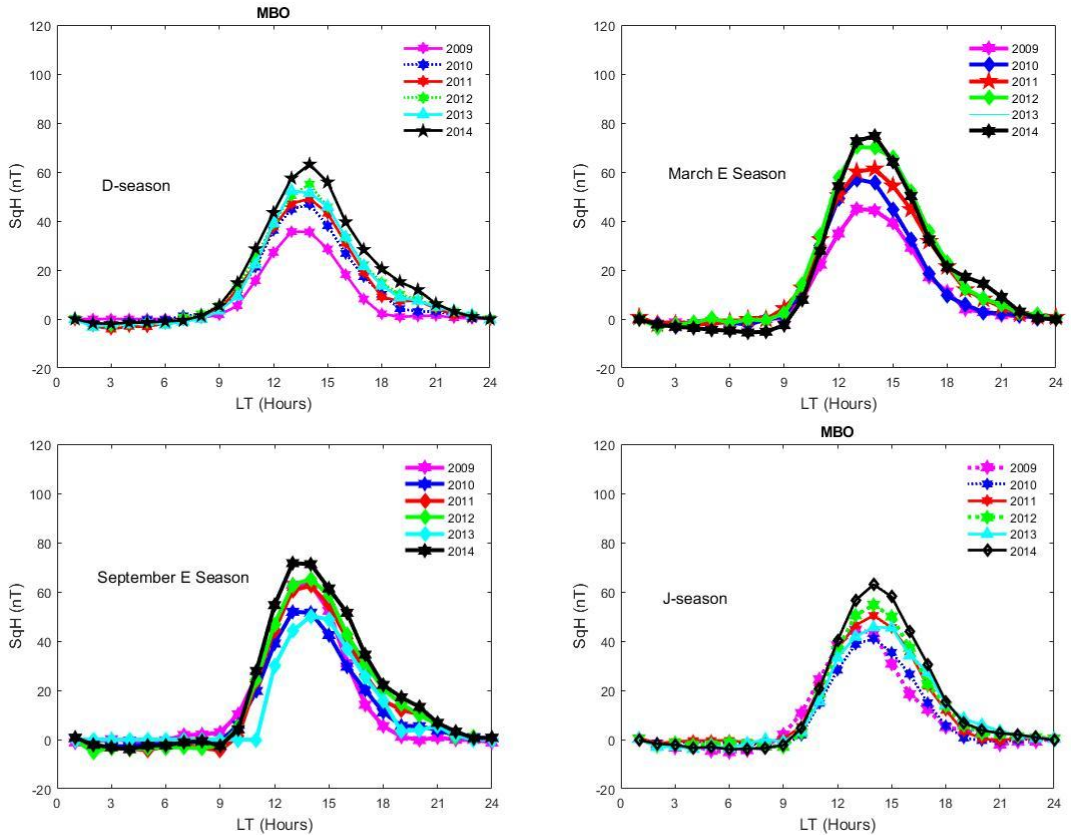

Figure 4.1.4: Seasonal variations of SqH at M'bour, Senegal from 2009 to 2014.

Mbour station is an EEJ station. It recorded a maximum SqH of about 78nT during March Equinox of 2014. The E-seasons recorded higher values than J and D seasons. The minimum peak of 45nT occurred in the year 2010 during the J season. The amplitude of the SqH seasonal

peaked between 1200LT to 1400LT for all the years under study in MBO. The daytime Sq peaks were observed to be higher than night time peaks since the rates of ionization are higher during the day than at night as indicated by figure 4.1.5. The afternoon to night values are constantly lower since the low solar intensity leading to low solar heating consequently leads to low ionization rates at these times. The SqH which represents currents in the ionosphere is produced by electron density; electron charge and the charge drift velocity. It is expected to be maximum at a point where there is an average of maximum electron density and drift velocity and since the maximum of drift velocity occurs at about 0900-1000LT while the maximum of electron density occurs at around noon, the SqH is expected to occur averagely around 1100LT though this adjusts with the solar heating towards noon.

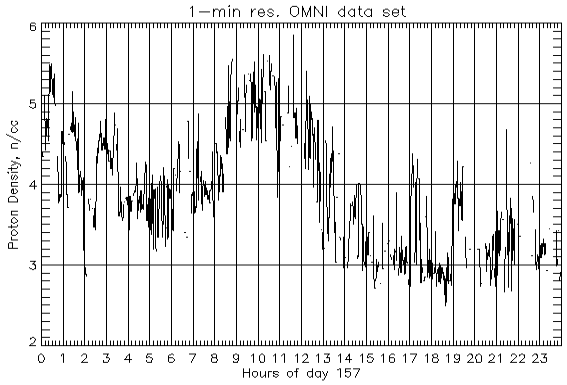

Figure 1.1.5: Variation of proton density with time of the day on 6th June ,2011.

In summary, the geomagnetic field is observed to exhibit a seasonal variation across all the stations under this study. The SqH exhibits roughly the same pattern for D, E and J season for the four stations with a maximum of the SqH around 110nT, 70nT, 65nT and 75nT for Addis Ababa, Yaoundé, Adigrat and Mbour respectively during the day. These maxima occur during E-seasons while the minimums occur during J seasons which is consistent with the findings of

(Yizengaw, et al., 2014) and (Fejer & Scherliess, 2001).The SqH magnitude is small in the D seasons and J seasons. The peak at Addis Ababa and Yaoundé stations occurs at local noon for all the seasons. This is attributed to the high ionization rates at around local noon in these stations. This is shown in Figure 4.1.5 above. The difference in peak time for sq seasonal variation is as a result of movement in the average position of the system of Sq current of electrojet in each season and the local wind electrodynamics. The peak at Adigrat occurs slightly before local noon in the E seasons but occurs at local noon during the D and J seasons while the peak at Mbour occurs between 1200LT- 1400LT for all the seasons. This is due to the effects of EEJ in Mbour. For Addis Ababa, the E- seasons both recorded the highest maxima in 2012 of around 110nT with peak at local noon. The minima for E-seasons were in 2010 of about 85nT. The highest for CMRN was observed in the year 2014 during the March equinox while the lowest peak for this station was recorded in the year 2010 during the J-season. For Adigrat station, the maximum peak occurred in the year 2012 during the March equinox while the minimum peak was in the year 2010 during the J-season. Adigrat station lacked data for the years 2009 and 2014. Finally, the peaks for Mbour are 78nT in March Equinox which was the maximum and 65nT during the D and J seasons as minimum. Like the other stations, it's also clear in MBO that the E-seasons recorded higher values of Sq than the J and D seasons. This was attributed to fact that during the equinoxes the rate of ionization is higher than in the J and D seasons as illustrated by Figure 4.2 on the proton density verses season of the year for the year 2011. The highest peaks were recorded in the year 2014 for all the seasons, followed by 2012 then 2011. This is consistent with the sunspot number progression Figure1.2.

This study realized that the morning values of Sq were smaller than evening values after the peak which occurred at around local noon. This is because the Sq is dependent on local time and as the time approaches noon there is increased ionization until around noon when it attains a peak value after which the values decrease towards evening again with decreasing ionization rates. (Ref. Figure 4.1.5).

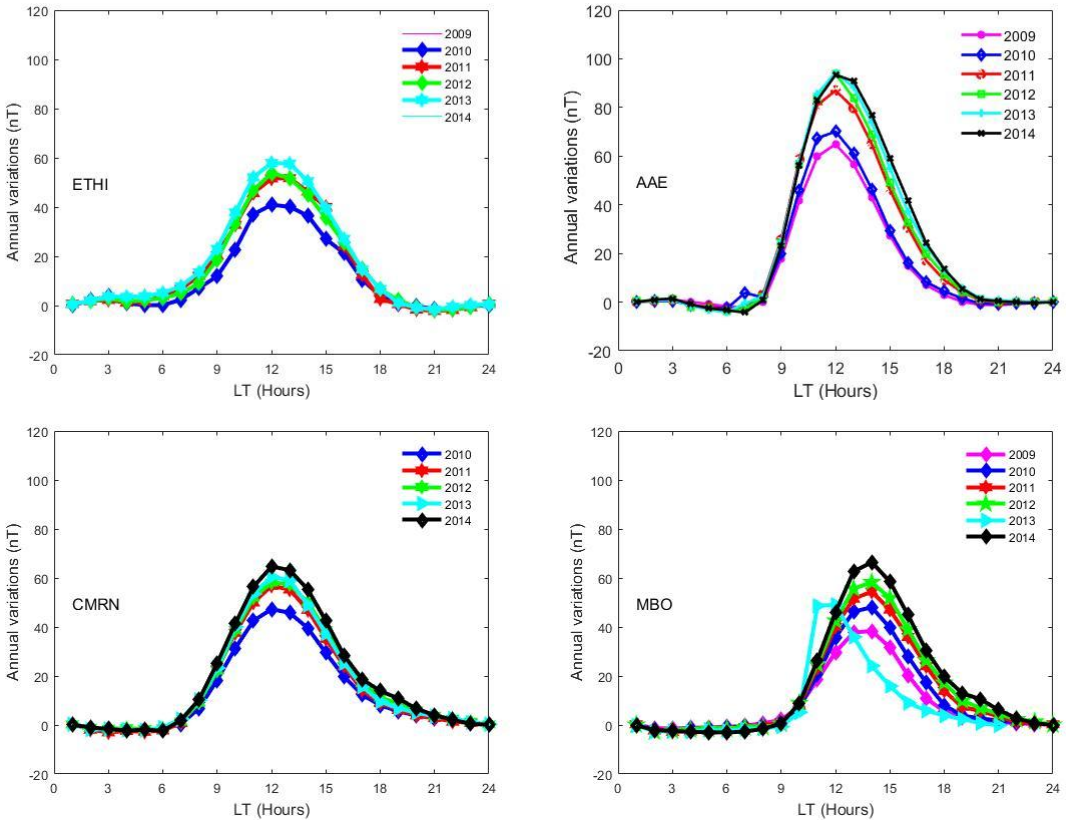

Figure 4.1.6: Annual variations of SqH at M'bour, Addis Ababa, Adigrat and Yaounde from 2009 to 2014.

The amplitude of the annual SqH shows local time dependence. There is a constant increase in amplitude from morning; a peak value is reached at about 1200LT followed by a gradual decrease to a minimum value of about 0nT attained during the evening hours. The highest values are recorded in the year 2014. The peaks at AAE and MBO, stations within the EEJ zone, are 98nT and 68nT respectively which are both higher than those for ETHI and CMRN, stations

outside the EEJ zone which are 58nT and 52nT respectively. This is because of the enhancement of Sq with the equatorial electrojet current at the EEJ region. The Sq magnitude at Adigrat, a station which is off the EEJ region is less than that at Addis Ababa which is within the EEJ region whereas the magnitude at Cameroon, a station off the EEJ region is also less than that at Mbour which is within the EEJ region. This is in agreement with the description of (Chapman S. , 1951) on how the daily range of the field of H component is intensified across the magnetic equator.

The annual variation is a function of solar activity as can be observed that the Sq value increases with the years for the ascending period of the solar cycle 24 from 2009 to 2014. This result concurs with the report of (Shinbori, Koyamana, Nose, Hori, Otsuka, & Yatagai, 2014); **(**Omondi**,** Baki**, &** Ndinya**,** 2016**).** From the results, it's also evident that the annual SqH values for AAE and ETHI are higher than those at MBO and CMRN. This observation is attributed to the longitudinal change of the geomagnetic major field that influences the non migratory tides. This is in agreement with the work of **(Abbas, Joshua, Bonde, & Gwani, 2013)**.

From the results of this study, it is observed that the magnitudes of SqH at the African equatorial region attains a peak at around local noon but the Sq values in the evening through the night up to early morning is generally around 0nT with the morning values lower than the evening values which are slightly greater than 0nT. This is attributed to a higher rate of ionization in the morning as the amplitude attains a peak with increasing solar heating as compared to a slower rate of recombination after the noon peak. The enhancement in the range of SqH observed in AAE and MBO is seen to be due to the EEJ current. This is because the two stations lie within the EEJ belt where the Eastward current consisting primarily of Hall current; EEJ and the Pederson current which is found in the set of the worldwide Sq current, overlap giving the total current.

4.2: Results and discussions of EEJ strength at Addis Ababa and Mbour stations

4.2.1: Annual variations of EEJ strength at AAE and MBO.

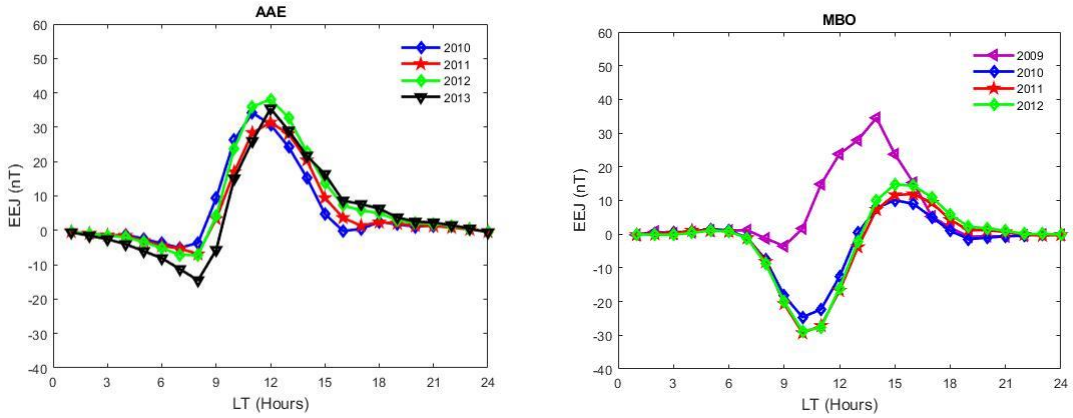

Figure 4.2.1: Annual variation in the EEJ strength for Addis Ababa and Mbour

The annual variation of EEJ strength had the highest peak of 40nT at local noon in Addis Ababa which occurred in the year 2012. The largest magnitude of EEJ strength was recorded in the 2012 which is a high solar activity year. This shows that annual EEJ strength is local time and solar activity dependent. The night (1800LT-0600LT) EEJ strength at Addis Ababa is around 0nT. The station also recorded a morning CEJ with a recorded maximum peak of about -15nT for the year 2013. The peak occurred at around 0900LT.

In Mbour, the maximum annual EEJ strength magnitude was recorded in 2009 with a peak of about 30nT. This year in Mbour showed a different trend as compared to the remaining years under study. This calls for further research. The daytime peaks occurred in the afternoon at around 1500LT. The rest of the years recorded daytime peaks of less than 20nT and the night time values were between 0-5nT. This also shows that EEJ annual variation is a function of solar activity and local time. However, Mbour station recorded high magnitudes of a morning CEJ at around 1000LT with maximum peak of 30nT recorded in the 2012.

The annual variation of EEJ indicates that the peaks at low solar activity years occurred slightly earlier than the peaks during high solar activity years. This may imply that when the solar activity is low, the ionization peak is attained earlier increasing the conductivity of the ionosphere.

In summary, the EEJ strength annual variations showed a longitudinal dependence with the peak value at Addis Ababa being higher at 40nT, than the values at Mbour which is about 20nT in the same year 2012. This is attributed to the fact that AAE (geomagnetic latitude 0.9^0) is much nearer to the dip equator than MBO (geomagnetic latitude 2.06^0) hence a greater enhancement of the EEJ current at AAE. At Addis Ababa, the magnetic variation is only 1.5^0E and the dip equator is aligned almost to the East. With the daily H component also directed almost to the North, then the direction of flow of the EEJ current is perpendicular to the magnetic variation. The EEJ at MBO peaks much later in the day at around 1500LT as compared to AAE where the peak occurs at around local noon. This is associated with the longitudinal variations of the Earth's main magnetic field which influences the non migratory tides. This longitudinal variation in the mean annual strength of EEJ agrees with the findings of (Rabiu, Yumoto, Falayi, Bello, & MAGDAS/CPNGroup, 2011), and (Yizengaw, et al., 2014) that, the strength of EEJ is greater as one moves to the Eastern African sector than to the West. They attributed this to a process of reinjection of energy to the electrojet as it flows eastwards. Sharp peaks are observed on some of the graphs which can be attributed to the irregularities arising from the inconsistent or poor data during some days for the given stations.

A morning Counter Electrojet was also observed for both stations with a maximum of about -30nT in Mbour in the year 2012 while that at Addis Ababa being about -15nT in the year 2013.The EEJ peak was higher in Addis Ababa while the CEJ peak was higher in Mbour as

compared to Addis Ababa. This is consistent with the findings of (Onwumecnihli, 1997) and (Rabiu, Olanike, Teiji, Nurul, & Yoshikawa, 2017) that the CEJ rarely occurs during periods when the EEJ is strong since the activities that support strong EEJ do inhibit occurrence of CEJ. These mechanisms include upward penetration of gravity waves from mesosphere to lower thermosphere region, appropriate phases combination of global scale tidal wind modes, influence of solar flares, changes in atmospheric temperatures associated with sudden stratospheric warming and changes in orientation of interplanetary magnetic field southward component B_Z. From the results it can be deduced that the EEJ strength mean annual variation depends on the sunspot number rising from 2009 towards 2014 as indicated by Figure 4.2.2, the strength increasing with the increase in the sunspot number. This means that the EEJ depends on the solar activity which increases the ionization rate of the ionosphere.

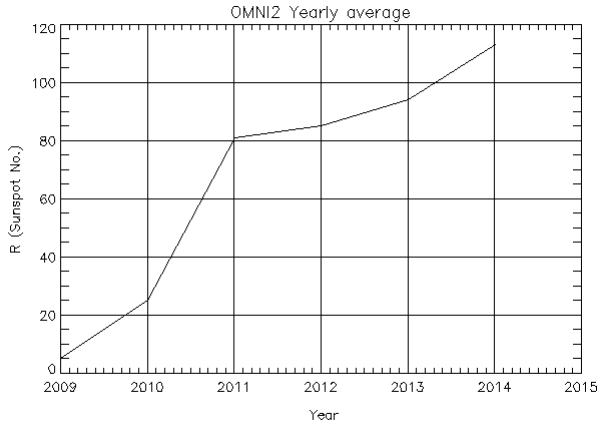

Figure 4.2.2: A graph of actual sunspot numbers from the year 2009 to 2014 (Administration, 2021) (Administration N. A., 2021)

4.2.2: Seasonal variations of EEJ strength at AAE and MBO

Figure 4.2.3 represents the results of the EEJ strength seasonal variation at AAE and MBO for

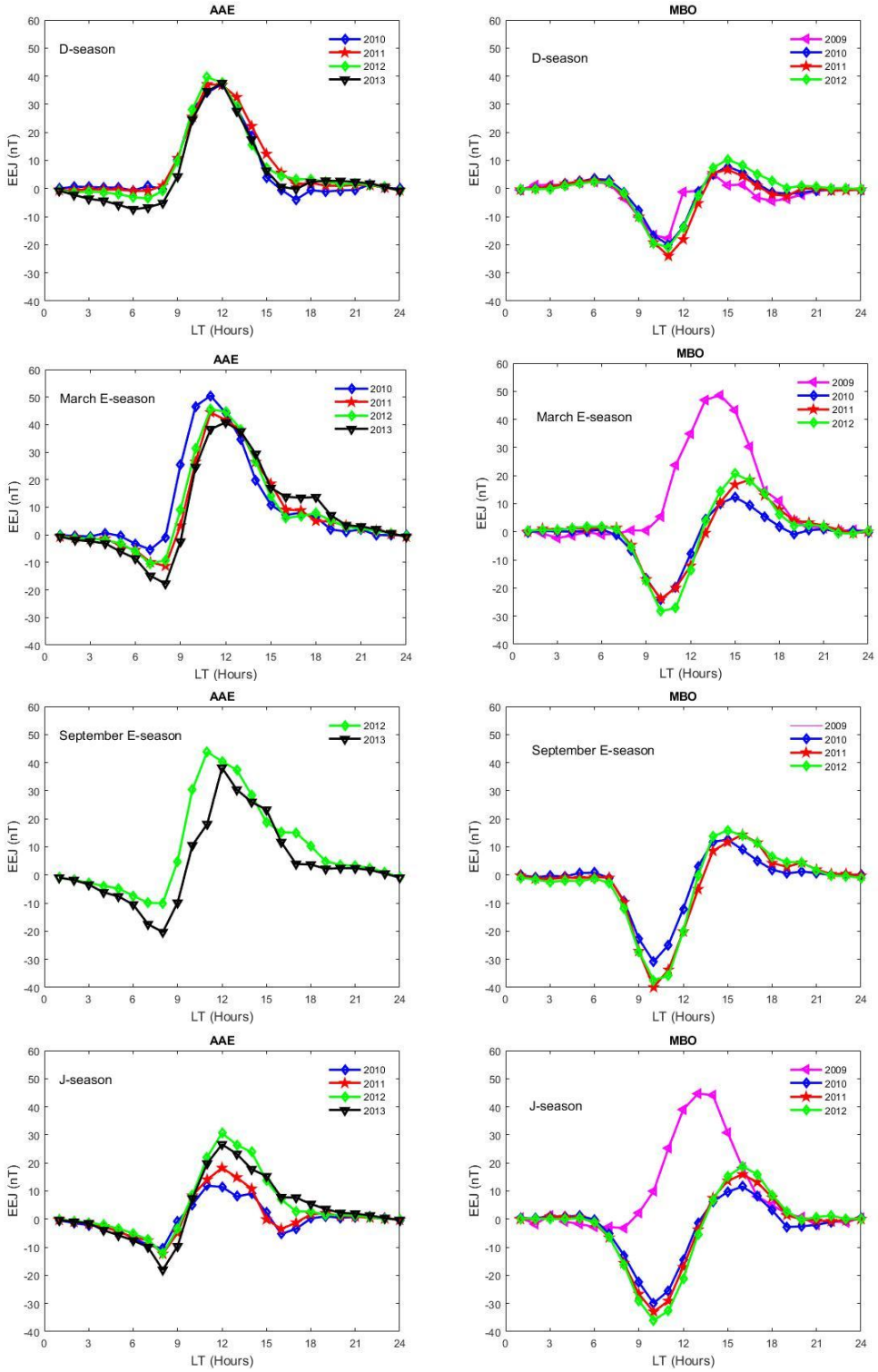

Figure 4.2.3: Seasonal variations of EEJ strength at AAE and MBO from 2009 to 2014.

Seasonal EEJ strength at Addis Ababa for December solstice, March Equinox, September Equinox and June solstice had maximum peak values of 42nT, 50nT,48nT and 35nT respectively, all occurring between 1000LT -1200LT. A morning CEJ ranging between -15nT and -20nT was also recorded for J season and the equinoxes respectively while the D season showed a CEJ magnitude of less than -10nT. The CEJs were observed between 0800LT and 0900LT. The night time amplitudes were quite low averaging between 0nT-5nT.

At Mbour, the EEJ magnitude peaks mainly in the afternoon between 1300LT and 1500LT with a maximum of 20nT for D and September Equinox. March Equinox and J season recorded maximum peaks of 50nT in the year 2009. This station also recorded morning CEJ occurring between 0900-1100LT. The maximum peaks for D, March E, and September E and J seasons were 25nT in 2011, 30nT in 2012, 40nT in 2011 and 35nT in 2012 respectively. The night time magnitudes were about 0nT.

Generally, from the results it is seen that EEJ was recorded in both AAE and MBO stations with AAE recording higher magnitudes as compared to MBO. AAE had morning EEJ while MBO had an afternoon EEJ with slightly lower magnitudes. This is an indication that EEJ exhibits a longitudinal variation attributed to the migratory tides fluctuations, diurnal tide propagations, local wind effects, and meridional winds effect as has been discussed by (Rabiu, OlufunmilayoFolarin, Uozumi, Hamid, & Yoshikawa, 2017) in their study of the longitudinal variability of the EEJ from one representative station up to another.

From Figure 4.2.3, it is also observed that both stations recorded a CEJ with AAE recording an early morning CEJ between 0600LT and 0900LTwhile MBO recorded CEJ in the late morning between 1000LT- 1100LT.The CEJ amplitude at MBO is larger than the amplitudes at AAE with

the largest peak at MBO being -40nT observed in the year 2011 during the September E season while the largest for AAE was -20nT in the year 2013 for both March and September E seasons. This indicates that CEJ also exhibits a longitudinal variation. While the magnitude of EEJ is greater in Addis Ababa than Mbour, the magnitude of CEJ is however greater in Mbour than in Addis Ababa implying that there could be an increased westward electric conductivity and high gradients in ionospheric conductivity during late morning hours in Mbour than in Addis Ababa. These factors that favor the occurrence of CEJ however oppose the occurrence of its EEJ. This is consistent with the findings of (Rabiu, OlufunmilayoFolarin, Uozumi, Hamid, & Yoshikawa, 2017).

This study has identified that both seasonal and annual peaks for EEJ at AAE occur at around local noon and the amplitudes are greater than the amplitudes at MBO which peaks much later. The late peak at Mbour can be ascribed to the effect of tidal winds and the variations in the geomagnetic main field. However, the CEJ at MBO peaks in the late morning and presents larger amplitudes than AAE which peaks much earlier. It therefore implies that EEJ occurring around noon has greater amplitudes attributed to higher ionization rates during this period; hence EEJ and CEJ are local time dependent phenomena.

4.3: Results and discussions on Storm time Variations of the Geomagnetic Field.

The magnetic field of the Earth also depicts a storm-time variation that was determined for selected days in this study. Table 3.2 shows the selected storm days and their corresponding maximum Kp values and highest negative Dst values. The data for the selected storm days were analyzed and the results recorded in Figure 4.3.1 and Figure 4.3.2.

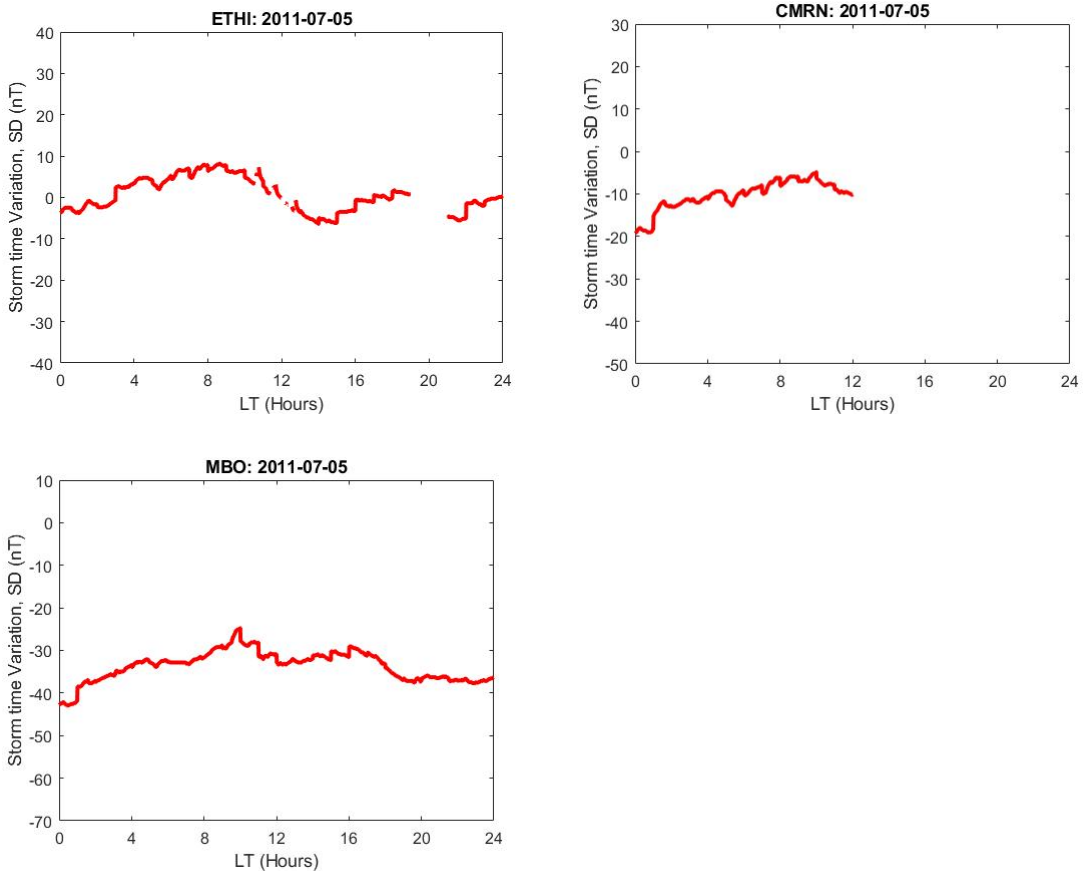

Figure 4.3.1: Storm time variations of the geomagnetic field on 5th July, 2011.

For ETHI, the storm of 5th July showed increasing values of S_D up to around 1100LT attaining a maximum value of 40nT. This was attributed to Storm Commencement (SC) after which there was recorded a rapid drop reaching a minimum value of -35nT at around 1400LT which was attributed to the storm's main phase. The beginning of the recovery phase was then observed towards the night hours past midnight. This storm of 5th July 2011 in CMRN, was at the recovery phase showing an increase in magnitude of S_D variation from -30nT at 0000LT to above 0nT at local noon. The discontinuous data for CMRN and AAE were as a result of data gaps for some days hours in the quiet or disturbed days selected for the study.

On July 16th, 2012, geomagnetic field storm variation at AAE showed a strong positive impulse in the local morning hours which is attributed to the storm commencement (SC). These values dropped rapidly, attaining a minimum value S_D of -170nT at around local noon. The variation was corresponded to the main phase of the storm. S_D then started increasing slowly attaining -10nT towards midnight. At CMRN the storm time variation had the same variation trend as that at Addis Ababa on the same day but with minimum amplitude of S_D of -130nT. The difference in these values can be linked to the effect of Equatorial Electrojet current at AAE and the influence of meridional winds and tidal waves at CMRN.

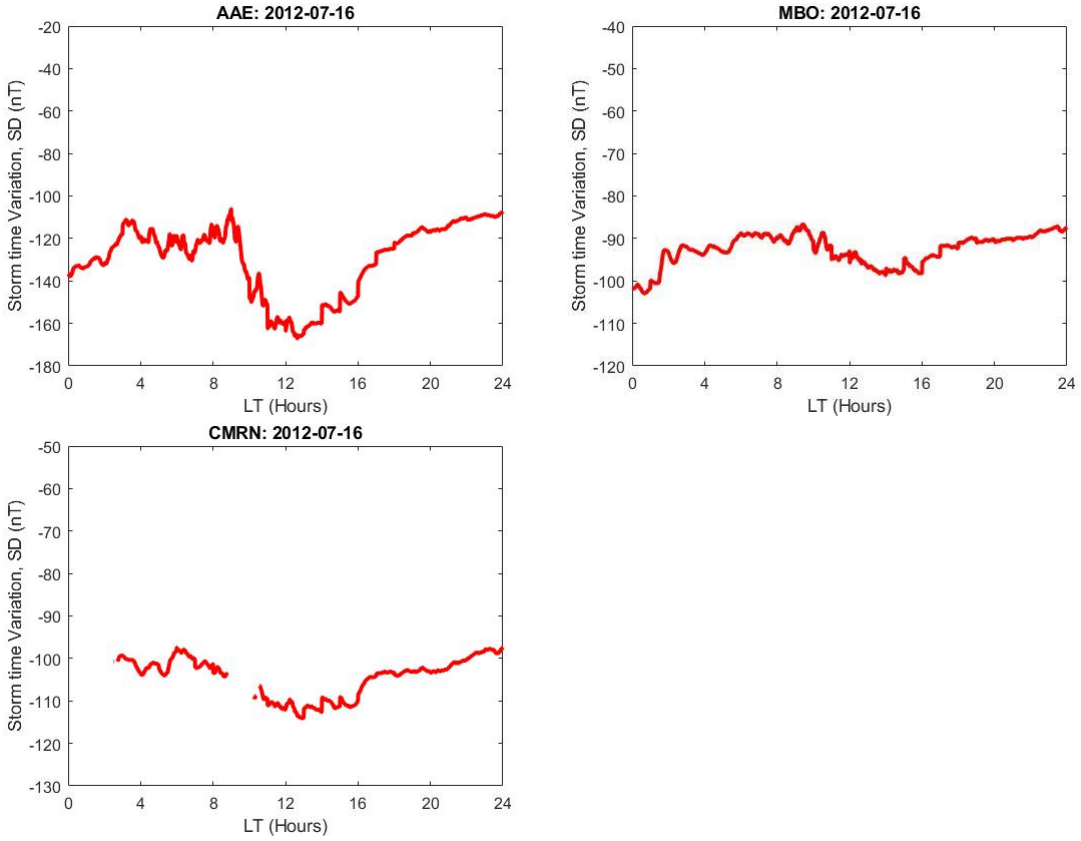

Figure 4.3.2: Storm time variations of geomagnetic field on 16th July, 2012.

35nT at around 1000LT then starts decreasing rapidly reaching a minimum value of -90nT at around 1400LT. This minimum is attributed to the second phase of the storm which is the main

phase. The variation trend then increases from around 1600LT towards the night time as it covers the final phase (recovery) of the storm. However the S_D values at MBO are slightly higher than those at CMRN with maximum value at during SC being around 30nT and the minimum attained at 2400LT at about -90nT. This is due to the fact that the EEJ at MBO enhances the effect of storms at this station.

Generally, the storm time variation showed an irregular and inconsistent pattern for all the stations under this study. This inconsistent pattern of variation was associated with the disturbance of the ionosphere which comes from sources without like the effects of space weather and effects of storms. The irregular perturbation electric fields deviates the geomagnetic field patterns from the quiet time patterns. The S_D values at the equatorial stations are observed to intensify with decreasing latitudes up to the dip equator showing that in addition to the magnetospheric ring currents, the effects of storms at the equatorial latitudes also depend on ionospheric currents like EEJ. Thus the equatorial magnetic storms are due to the combined effects of disturbance ring currents and the IMF.

CHAPTER FIVE

SUMMARY, CONCLUSIONS AND RECOMMENDATIONS

5.1 Introduction

In this chapter, a summary of main findings of this work is given, the practical applications and implications of these findings in real life discussed and recommendations for further research made.

5.2 Summary

This study was set forth to characterize the variations of the magnetic field of the Earth at the equatorial regions of Africa during the Ascending phase of the solar cycle 24 by finding the solar quiet seasonal and annual variations and storm time variations of the Earth's magnetic field for the equatorial stations; Addis Ababa, Adigrat Yaoundé and Mbour in the period from the year 2009 to 2014. The EEJ strength at Addis Ababa and Mbour stations was also estimated for the same period. The data used was obtained from ground based magnetometers from the stations under study which was analyzed and results discussed.

In summary, this study has made the following new contributions to knowledge:

(i) The annual variation of EEJ strength at African equatorial regions indicates that the peaks at low solar activity years occurred between 1100LT-1130LT which is slightly earlier than the peaks during high solar activity years which occurred at local noon.

(ii) Storm time variation of the geomagnetic field has a latitudinal dependence at the equatorial region with the intensity of the ring current increasing towards the dip equator as shown by the high negative peaks of S_D at the stations closest to the dip equator.

(iii) The morning values of Sq were smaller than evening values after the peak which occurred at around local noon because of ionization. It takes longer for recombination to occur than for dissociation. The conclusions from the findings are given in Section 5.2.

5.3 Conclusions

5.3.1 Conclusions on Solar quiet seasonal and annual variations

i. For the African equatorial region, the equinoctial peaks of SqH are generally higher than the peaks during the D and J seasons. The largest seasonal Sq values were observed during the March equinox and December equinox in the year 2014 while the largest annual values were observed in the year 2014.

ii. There is a solar activity and a dependence on the local time for the annual geomagnetic field variation in Sq. The Sq magnitude increases with increasing activity of the sun, with the highest attained amplitudes in the years of 2012 and 2014 which were high solar activity years. The daily peaks were seen at around local noon for all the stations under this study.

iii. The maximum peaks during the years when the solar activity was low occurred slightly earlier than peaks during high years when it was high.

5.3.2 Conclusions on Estimation of EEJ strength

i. The Addis Ababa and Adigrat showed a large peak of EEJ with a very small peak of CEJ while Yaoundé and Mbour station displayed a large CEJ peak and a small EEJ peak.

ii. EEJ exhibits a longitudinal variation.

iii. The morning CEJ is recorded in the African equatorial region which does not show seasonal variation as the EEJ does.

EEJ around local noon and CEJ occurring in the late morning have greater amplitudes as compared to those in the early morning and afternoon. This shows that EEJ depends on local time of the day and ionization rate.

5.3.3 Conclusions on storm time variation

i. Storm time variation has a latitudinal dependence at the equatorial region with perturbation magnitude increasing to the lowest negative at the dip equator.

5.4 Recommendations to Industry and Research Community

i) The space agencies and African governments and other researchers can use the results of this study as a basis to make long term forecasts on the impact of storms in order to mitigate or reduce their effect on the economic and ecological environment.

ii) In this study the Earth's magnetic field magnitude variations were analyzed. This is useful to aviation industry in helping to improve the air travel safety since this data from African equatorial regions can be included in the global database for high-precision navigation underground which is usually based upon continuous quantification of the geomagnetic field.

5.5 Suggestions for further research.

(i) This study identified that the storm time variations may depict a latitudinal variation in the African equatorial regions since there is intensified amplitudes at AAE which is closest to the Dip equator than MBO,CMRN and ETHI and recommends that future researches investigate into this for the inclining phase of solar cycle 24.

(ii) It also suggests further research on the tidal trends in the African equatorial regions to further establish their effect on the geomagnetic field variations in this region and for further understanding of the late peaks of both EEJ and Sq in Mbour and Yaoundé as compared to Addis Ababa and Adigrat.

(iii)This study also recommends further research using alternative methods to ascertain the observation that the morning CEJ is recorded in the African equatorial region which does not show seasonal variation in the inclining period of solar cycle 24 and establish a possible reason for this.

REFERENCES

National Oceanic and Atmospheric Administration. (2020). *www.ngdc.noaa.gov*. Retrieved 2021, from Https://www.ngdc.noaa.gov/geomag/geomaginfo.shml

Abbas, M., Joshua, B., Bonde, D., & Gwani, M. (2013). Longitudinal and Seasonal Variation along the magnetic Equator Using MAGDAS/CPMN. *International Journal of Marine ,Atmospheric and Earth Sciences* , 8-16.

Abbas, M., Joshua, B., Bonde, D., Adimula, I. A., Rabiu, A. B., & Bello, O. R. (2012). Variability of electrojet strength along the magnetic equator using MAGDAS/ CPMN data. *INFORMATION AND DATA MANAGEMENT* .

Adebesin, B., & Yumoto, K. (2013). F2 layer characteristics and electrojet strength over an equatorial station. *Advances in Space Research , 52* (5), 791-800.

Adimula, I., & Akpaneno, A. (2015, February 20). Variabilities of H- component of the Geomagnetic field from some Equatorial Electrojet stations. *Sun and Geosphere* , pp. 67-77.

Administration, N. A. (2021, March 21). *OMNIweb*. Retrieved August 30, 2021, from GODDARD SPACE FLIGHT CENTRE, Space Physics Data Facility: omniweb.gstc.nasa.gov/html/ow_data.html

Archana, R. K., & Arora, K. (2022). Variations of Sq foci position from the indian longitudes and its influence on Equatorial Electrojet. *Atmospheric and Solar- Terrestrial physics , 236*, 105911.

Babayev, E. S., & Allahverdiyeva, A. A. (2007). Effects of geomagnetic activity variations on the physiological state of functionally healthy humans. *Advances in Space Research , 40* (12), 1941-1951.

Baumjohann, W., & Treumann, R. A. (1960). Basic space plasma physics. *London:Imperial college press* .

Chapman, & Bartels. (1940). Geomagnetism. *Oxford university press* , 1049.

Chapman, S. (1951). The equatorial Electrojet as detected from the abnormal electric current distribution above Huancayo, Peru, and elsewhere. *Arch. Meterol. Geophys. , 4*, 368-39.

Chiaha, S. O., Ugonabo, O. J., & Okpala, K. C. (2019). A study on the effects of solar wind and interplanetary magnetic field on geomagnetic H-component during geomagnetic storms. *International Journal of Physical Sciences* , 38 -44.

Haile, T. (2003). equatorial electrjet strength in the african sector during high and low activity years. *short communication* .

Haines, C., & Owens, M. J. (2019). Variation of Geomagnetic Storm duration with Intensity. *Solar physics* , 294.

Idowu, A. O., Adimula, I. A., & Adebesin, B. O. (2020). Variations in equatorial electrojet current along the 210A degrees MM chain: Comparison of two approaches. *International Journal of Physical Sciences , 15* (3), 120-129.

Idowu, A., & Adimula, A. (2020). Characterization of magnetic field horizontal component in selected stations along the 210 degree MM. *Nigeria Journal of Pure and Applied Physics , 10* (1), 16-19.

Iyemori, T. (1990). Storm-time magnetospheric Currents Inferred from Mid-latitude Geomagnetic Field Variations. *Journal of geomagnetism and geoelectricity. , 42* (11), 1249-1265.

Lin, J. W. (2021). Geomagnetic Storm Related to Disturbance Storm Time Indices. *European Journal of of Enviroonment and Earth Scinces , 2* (6), 102-199.

Maeda, H. (1968). Variation of Geomagnetic Field. *Space Science Reviews , 8* (4), 555-590.

Mandrikova, O. V., Solovev, I. S., & Zalyaev, T. L. (2014). Methods of Analysis of Geomagnetic field Variations and Cosmic ray data. *Earth, Planet and Space* , 66.

Manoj, C., Luhr, H., Maus, S., & N.Nagarajan. (2006). Evidence for short spartial correlation lengths of the noontime equatorial electrojet inferred from a comparison of satellite and ground magnetic data. *Geophysical Research* , 111.

Mayaud, P. N. (1980). Derivation, Meaning and Use of Geomagnetic Indices. *Washington DC American Geophysical Union Geophysical Monograph series 22* .

Mungufeni, P., Habarulema, J. B., Orue, Y. M., & Jurua, E. (2018). Statistical Analysis of the correlation between the equatorial elecrojet and the occurrence of the equatorial ionization anomaly over the East African sector. *Annales Geophysicae , 36* (3), 841-853.

Narang, S., Gupta, M., & Gaur, A. S. (2016). The Study of Present Solar Cycle 24- Future Aspects. *Research journal of physical sciencesvol.4(3)* , 5-10.

NOAA. (2021, March 9th). *SOLAR CYCLE PROGRESSION*. Retrieved April 16th, 2021, from https://www.swpc.noaa.gov.

Obiekezie, T. N. (2012). Geomagnetic Field variations at dip Equatorial latitudes of West Africa. *International Journal of physical sciences* , 5372-5377.

Okeke, F. N., & Hamano, Y. (2000). Daily variations of geomagnetic H, D and Z field at Equatorial latitudes. *Earth, Planet and Space* , 237-243.

Okeke, F. N., Onwumechili, C. A., & Rabiu, B. A. (1998). Day-to-day variability of geomagnetic hourly amplitudes at low latitudes. *Geophysicae Journal Internationale* , 484-500.

Omondi, G., Baki, P., & Ndinya, B. (2016). Quiet Time Geomagnetic Field Variations in the Equatorial East African Region During the Inclining phase of Solar Cycle 24. *International Journal of Astrophysics and Space Science.* , 21-25.

Onwumecnihli, C. A. (1997). The Equatorial Electrojet. *Gordon and Breach Science publisher* .

Owens, M. J., Lockwood, M., Hawkwins, E., Usoskin, I., S, G., Barnad, L., et al. (2017). The Maunder minimum and the Little Ice Age: an update from recent reconstructions and climate simulations. *Space weather and Space climate* .

Owolabi, Rabiu, Olayanju, G. M., & Bolaji. (2014). Seasonal Variation of Worlwide Solar Quiet of the Horizontal Magnetic Field Intensity. *Applied Physics Research; vol.6(2)* , 82.

Rabiu, A. B., Mamukuyomi, A. I., & Joshua, E. O. (2007). Variability of equatorial ionosphere inferred from geomagnetic field measurements. *Bulletin of the Astronomical Society of India* , 607-618.

Rabiu, A. B., Olanike, O. F., Teiji, U., Nurul, S. A., & Yoshikawa, A. (2017). Longitudinal Variation of equatorial electrojet and the occurrence of its couter electrjet. *Annales Geophysicae , 35*, 535-545.

Rabiu, A. B., OlufunmilayoFolarin, O., Uozumi, T., Hamid, N. S., & Yoshikawa, A. (2017). Longitudinal Variation of Equatorial Electrojet and the occurrence of its Counter Electrojet. *Annales Geophysicae , 35*, 535- 545.

Rabiu, A. B., Yumoto, K., Falayi, E. O., Bello, O. R., & MAGDAS/CPNGroup. (2011). Ionosphere over Africa: Results from geomagnetic field measurements during international Heliophysical YearIHY. *Journal of Sun and Geosphere , 6*, 61-64.

Rabiu, B. A., Nagarajan, N., Okeke, F. N., & Ayiribi, A. E. (2007). variability of equaatorial ionosphere infered from geomagnetic field measurements. *A journal of science and technology vol. 8 No. 2* , 609.

Ranasinghe, M., Fujimoto, A., & Jayarante, C. (2021). seasonal variation of inter-hemispheric field -aligned currents deduced from time series analysis of the equatorial geomagnetic field data during solar cycle 23-24. *Earth, Planets and Space* , 146.

Rastogi, R. G., Kitamura, T., & Kitamura, K. (2004, September). Geomagnetic field variations at the equatorial electrojet station in Sri Lanka, Peredinia. *Annales Geophysicae* , pp. 2729-2739.

Rastogi, R. G., Kitamura, T., & Kitamura, K. (2004). Geomagnetic Field Variations at the Equatorial Electrojet station in Sri Lanka, Peredinia. *Annales Geophysicae* , 2729-2739.

Rastogi, R., & Trivedi, N. (2009). Asymmetries in the equatorial electrojet around N-E Brazil sector. *Annales Geophysicae* , 1233-1249.

Rawat, R., Echer, E., & Gonzalez, W. D. (2018). How different are the solar wind-interplanetary conditions and the consequent Geomagnetic activity during the Ascending and early Descending phases of the Solar cycles 23 and 24? *Geophysical Research: Space Physics* , 6621-6638.

Shailraj Narang, M. G. (2016). The Study of Present Solar Cycle 24- Future Aspects. *Research journal of Physical Sciences vol.4(3)* , 5-10.

Shinbori, A., Koyamana, Y., Nose, M., Hori, T., Otsuka, Y., & Yatagai, A. (2014). Long-term variation in the upper atmosphere as seen in the geomagnetic solar quiet daily variation. *Earth, Planets and Space , 66* (1), 155.

Silva, A. A., Yamaguti, W., Kuga, H. K., & Celestino, C. C. (2012). Assessment of the Ionospheric and Tropospheric Effects in Location Errors of Data Collection platforms in Equatorial regions during high and low Solar Activity periods. *Mathematical Problems in Engineering , 4*, 3-5.

Tuo, Z., Doumbia, V., Coisson, P., & etal. (2020). variations of the peak positions in the longitudinal profile of noontime equatorial electrojet. *Earth Planets Space , 72*, 174.

Watani, S. (2017). Geomagnetic Storms of Cycle 24 and their solar sources. *Earth, Planets and Space* .

Watermann, J., & Gleisner, H. (2009). Geomagnetic Variations and their time derivatives during geomagnetic storms at different levels of Intensity. *Acta Geophysica , 57* (1), 197-208.

Yamazaki, Y., Richmond, A. D., Liu, N., Pedatella, N., Maute, A., & Sassi, F. (2014). Day -to-day variation of the equatorial electrojet during quiet periods. *Journal of Geophysical Research on Space physics* , 6966-6980.

Yizengaw, E., Moldwin, M. B., Zesta, E., Biouele, C. M., Damtie, B., Mebrahtu, A., et al. (2014). The longitudinal variability of equatorial electrojet and vertical drift velocity in the African and American sectors. *Annales Geophysicae , 32*, 231-238.

Zhang, K., Wang, W., Wang, H., Dang, T., Liu, J., & Wu, Q. (2018). The longitudinal variations of upper thermospheric zonal winds observed by the CHAMP satelite at low and midlatitudes. *Journal of Geophysical Research : Space Physics* , 9652-9668.

APPENDICES

APPENDIX I: A SCRIPT TO CALCULATE THE HORIZONTAL COMPONENT OF A MAGNETOMETER STATION IN AN EQUATORIAL ELECTROJET BELT USING INTERMAGNET DATA

```
%This function calculates the horizontal component of a magnetometer
% station in an equatorial electrojet belt eg. AdisAbbaba using
% INTERMAGNET data
clear
clc
%
% datapath = '/home/habyarimana/Lucy_revised/Magnetometer_data/';
% cd(datapath)
%
% data=dir('aae2014*.min');
% H_value_inside_EEJ=[];
%
% for k=1:length(data)
%     filename=data(k).name;
%     fid=fopen(filename);
%
%     Data = textscan(fid,'%s %s %f %f %f %f %f','headerlines',26);
%
%     Year = str2num(filename(4:7));
%     doy = Data{3};
%     Xcpt = Data{4};
%     Ycpt = Data{5};
%     Times = Data{2};
%     time = cell2mat(Times);
%
%     Time = [];
%     for ij = 1:length(time)
%         Hr = str2num(time(ij,1:2));
%         Mnt = str2num(time(ij,4:5));
%         Timer = [Hr*60 + Mnt];
%         Time = [Time;Timer];
%     end
%
%     Req_data = [repmat(Year,size(doy)) doy Time XcptYcpt];
%
%     for ii = 1:length(Req_data)
```

```
%        ind = find(Req_data(ii,4)== -9999 | Req_data(ii,5)  == -9999);
%        Req_data(ind,4)= NaN;
%        Req_data(ind,5)= NaN;
%    end
%
%    Hc = sqrt(Xcpt.^2 + Ycpt.^2);
%
%    DATA = [Req_data(:,1:3) Hc];
%
%    H_value_inside_EEJ = [H_value_inside_EEJ;DATA];
% end
%
% binwidth = 0:1:24;
% Hourly_H_value_inside_EEJ = [];
% for ii = 1:length(binwidth)-1
%    ind = find(H_value_inside_EEJ(:,3)>= binwidth(ii)
&H_value_inside_EEJ(:,3)<binwidth(ii+1));
%    Req_H_value_inside_EEJ = nanmean(H_value_inside_EEJ(ind,4));
%    Hourly_H_value_inside_EEJ = [Hourly_H_value_inside_EEJ;Req_H_value_inside_EEJ];
% end
%
% H1 =
[Hourly_H_value_inside_EEJ(1,:);Hourly_H_value_inside_EEJ(2,:);Hourly_H_value_inside_E
EJ(23,:);Hourly_H_value_inside_EEJ(24,:)];
% H0 =nanmean(H1) ;
% HO = ones(24,1)*H0;
% Hourly_departures = Hourly_H_value_inside_EEJ - HO;
% Delta_C = ((Hourly_departures(1,:)- Hourly_departures(24,:)))/23;
%
% sq2 = [];
%  for t=1:1:24
%    Sq = Hourly_departures(t,:)+(t-1)*Delta_C;
%    sq2 = [sq2;Sq];
%  end
%
%  Hourly_values = [repelem(Year,24,1) repelem(unique(doy),24,1) (1:1:length(binwidth)-1)'
Hourly_H_value_inside_EEJ sq2];
%  fout = '/home/habyarimana/Lucy_revised/H_sq2_inside_EEJ_aae_2014.txt';
%  dlmwrite(fout, Hourly_values, '\t')
%
```

```
% ahaha
 %% Seasonal classification according to Lloyd

 datapath1 = '/home/habyarimana/Lucy_revised/';
cd(datapath1)

Hourly_values = load('H_sq2_inside_EEJ_aae.txt');

%  D_season = [November December January February];
%  E_season_March = [March April];
%  J_season = [May June July August];
%  E_season_September = [September October];


year = 2009:1:2014;

All_D_season = [];
All_E_season_March = [];
All_J_season = [];
All_E_season_September = [];


for ii = 1:length(year)

index = find(Hourly_values(:,1)== year(ii));
   Datum = Hourly_values(index,:);

if mod(year(ii),4)==0
season_ends = [0 60 121 244 305 366];
      index1 = find(Datum(:,2)> 0 & Datum(:,2)<= 60 | Datum(:,2)> 305 & Datum(:,2)<= 366);
      index2 = find(Datum(:,2)> 60 & Datum(:,2)<= 121);
      index3 = find(Datum(:,2)> 121 & Datum(:,2)<= 244);
      index4 = find(Datum(:,2)> 244 & Datum(:,2)<= 305);
else
season_ends = [0 59 120 243 304 365];
      index1 = find(Datum(:,2)> 0 & Datum(:,2)<= 59 | Datum(:,2)> 304 & Datum(:,2)<= 365);
      index2 = find(Datum(:,2)> 59 & Datum(:,2)<= 120);
      index3 = find(Datum(:,2)> 120 & Datum(:,2)<= 243);
      index4 = find(Datum(:,2)> 243 & Datum(:,2)<= 304);
end
```

```
D_season = Datum(index1,:);
E_season_March = Datum(index2,:);
J_season = Datum(index3,:);
E_season_September = Datum(index4,:);

All_D_season = [All_D_season;D_season];
All_E_season_March = [All_E_season_March;E_season_March];
All_J_season = [All_J_season;J_season];
All_E_season_September = [All_E_season_September;E_season_September];
end

All_seasonal_data =
[All_D_seasonAll_E_season_MarchAll_J_seasonAll_E_season_September];
fout1 = '/home/habyarimana/Lucy_revised/All_seasonal_data_DMJS_aae.txt';
dlmwrite(fout1, All_seasonal_data, '\t')

%% Selecting geomagnetically quiet days in a month based on Kp less or equal to 2

filename=sprintf('kp_index.txt'); % name of file that contains Kp values
Fid=fopen(filename);

fori= 1% loop to count header lines
   Line=fgetl(Fid);
end
Dat=[]; Count=1; % allocating memory for storing kp data
while 1
    Line= fgetl(Fid);
if Line == -1, break, end% end of the line
yyyy = str2num(Line(1:4));
mm = str2num(Line(5:6));
dd = str2num(Line(7:8));
%       Date = str2num(Line(1:8));
     Date = [yyyy mm dd] ;

     Dat1= str2num(Line(10)); Dat2=str2num(Line(12)); Dat3= str2num(Line(14));Dat4=
str2num(Line(16));
     Dat5= str2num(Line(18));Dat6= str2num(Line(20));Dat7= str2num(Line(22));Dat8=
str2num(Line(24));
     Dat0=[Date repelem(Dat1,3) repelem(Dat2,3) repelem(Dat3,3) repelem(Dat4,3)
repelem(Dat5,3) repelem(Dat6,3) repelem(Dat7,3) repelem(Dat8,3)];
```

```
Dat=[Dat;Dat0];
end

Quiet_days = [];
forij = 1:length(Dat)
%      index5 = find(max(Dat(ij,2:25))==2); %Finding a quiet day
    index5 = find(max(Dat(ij,4:27))==2); %Finding a quiet day
if index5==1
Quiet_day = Dat(ij,:);
else
continue
end
Quiet_days = [Quiet_days;Quiet_day];
end

 %% Converting the Quiet days to doy
doys = [];
forih = 1:length(Quiet_days)
   x = datetime(Quiet_days(ih,1),Quiet_days(ih,2),Quiet_days(ih,3));
doy = day(x,'dayofyear');
doys = [doys; doy];
end

Quiet_days_data = [Quiet_days(:,1) doys];

%% Selecting disturbed days from the data using Dst<=-50 nT

Dst_data = dlmread('Dst_Kp_index_omni.txt','',10,0);

days = unique(Dst_data(:,1:2),'rows');

Disturbed_days = [];
foril = 1:length(days)
   index9 = find(Dst_data(:,1)==days(il,1) &Dst_data(:,2)==days(il,2));
Dst_datum = Dst_data(index9,:);
   index10 = find(max(Dst_datum(:,5)==-50));
if index10==1
Disturbed_day = days(il,:);
else
continue
```

```
end
Disturbed_days = [Disturbed_days;Disturbed_day];
end

%% Selecting Sq for quiet days and averaging per month and subtracting it from H values of
disturbed days

index6 = find(ismember(Hourly_values(:,1:2), Quiet_days_data(:,1:2),'rows'));

Required_hourly_values = Hourly_values(index6,:);

index12 = find(ismember(Hourly_values(:,1:2), Disturbed_days(:,1:2),'rows'));

Required_hourly_disturbed_values = Hourly_values(index12,:);

Disturbed_daily_variation_intermagnet = [];

for ii = 1:length(year)

   index7 = find(Required_hourly_values(:,1)== year(ii));
Datums = Required_hourly_values(index7,:);

   index13 = find(Required_hourly_disturbed_values(:,1)==year(ii));
Disturbed_datum = Required_hourly_disturbed_values(index13,:); % Data for H component for
disturbed days

if mod(year,4)==0
months_ends = [0 31 60 91 121 152 182 213 244 274 305 335 366];
else
months_ends = [0 31 59 90 120 151 181 212 243 273 304 334 365];
end

All_disturbed_daily = [];
forik = 1:length(months_ends(1,:))-1
      index8 = find(Datums(:,2)>months_ends(ik) &Datums(:,2)<= months_ends(ik+1));
Req_data_per_month = nanmean(Datums(index8,5)); % monthly mean sq value

      index11 = find(Disturbed_datum(:,2)>months_ends(ik) &Disturbed_datum(:,2)<=
months_ends(ik+1));
```

```
Disturbed_data_per_month = Disturbed_datum(index11,4); % Data for H component for
disturbed days
Disturbed_daily = Disturbed_data_per_month - Req_data_per_month;
All_disturbed_daily = [All_disturbed_daily;Disturbed_daily];
end
Disturbed_daily_variation_intermagnet = [year(ii) All_disturbed_daily];
end

fout2 = '/home/habyarimana/Lucy_revised/Disturbed_daily_variation_intermagnet.txt';
dlmwrite(fout2, Disturbed_daily_variation_intermagnet, '\t');
```

.

APPENDIX II: ASCRIPT TO CALCULATE THE HORIZONTAL COMPONENT OF A MAGNETOMETER STATION OUTSIDE THE EQUATORIAL ELECTROJET BELT USING AMBER DATA

```
clear
clc

datapath = '/home/habyarimana/Lucy_revised/';
cd(datapath)

data = load('All_H_value_outside_EEJ_ETHI.txt');

index = find(~isnan(data(:,4)));

H_value_outside_EEJ =  data(index,:);

%% %% Selecting geomagnetically quiet days in a month based on Kp less or equal to 2

filename=sprintf('kp_index.txt'); % name of file that contains Kp values
Fid=fopen(filename);

for i= 1% loop to count header lines
    Line=fgetl(Fid);
end
Dat=[]; Count=1; % allocating memory for storing kp data
 while 1
     Line= fgetl(Fid);
      if Line == -1, break, end % end of the line
      yyyy = str2num(Line(1:4));
      mm = str2num(Line(5:6));
      dd = str2num(Line(7:8));
%       Date = str2num(Line(1:8));
      Date = [yyyy mm dd] ;

      Dat1= str2num(Line(10)); Dat2=str2num(Line(12)); Dat3= str2num(Line(14));Dat4=
str2num(Line(16));
      Dat5= str2num(Line(18));Dat6= str2num(Line(20));Dat7= str2num(Line(22));Dat8=
str2num(Line(24));
      Dat0=[Date repelem(Dat1,3) repelem(Dat2,3) repelem(Dat3,3) repelem(Dat4,3)
repelem(Dat5,3) repelem(Dat6,3) repelem(Dat7,3) repelem(Dat8,3)];
      Dat=[Dat;Dat0];
 end

 Quiet_days = [];
 for ij = 1:length(Dat)
%      index5 = find(max(Dat(ij,2:25))==2); %Finding a quiet day
     index5 = find(max(Dat(ij,4:27))==2); %Finding a quiet day
     if index5==1
        Quiet_day = Dat(ij,:);
     else
         continue
     end
     Quiet_days = [Quiet_days;Quiet_day];
 end

 %% Converting the Quiet days to doy
```

APPENDIX III: A SCRIPT TO PLOT Sq ANNUAL DATA PER YEAR FOR ALL THE FOUR STATIONS ON THE SAME GRAPH

```
% This script plots mean annual data per year for all the four stations on
% the same graph

clear
clc

datapath = '/home/habyarimana/Lucy_revised/SqH/All_annual_data/';
cd(datapath)

year = 2009:1:2014;

for ii = 1:length(year)
    data1 = load(['All_annual_sqH' sprintf('%d',year(ii)) '_AAE.txt']);
    data2 = load(['All_annual_sqH' sprintf('%d',year(ii)) '_CMRN.txt']);
    data3 = load(['All_annual_sqH' sprintf('%d',year(ii)) '_ETHI.txt']);
    data4 = load(['All_annual_sqH' sprintf('%d',year(ii)) '_MBO.txt']);

    a = plot(nanmean(data1,2),'m');
    hold on
    b = plot(nanmean(data2,2),'b');
    hold on
    c = plot(nanmean(data3,2),'r');
    hold on
    d = plot(nanmean(data4,2),'g');

    h = legend([a;b;c;d],{'AAE','CMRN','ETHI','MBO'});
    set(h,'Orientation','vertical','box','off','Location','northeast');

    xlim([0 24])
    set(gca,'XTick',[0 3 6 9 12 15 18 21 24]);
    ylabel('SqH (nT)', 'Fontsize',12)
    xlabel('LT (Hours)', 'Fontsize',12)
    text(1,0,sprintf('%d',year(ii)),'Fontsize',12)

saveas(gcf,['/home/habyarimana/Lucy_revised/SqH/All_stations/All_stations_'
sprintf('%d',year(ii))],'fig');
    close
end
```

APPENDIX IV: ASCRIPT TO PLOT EEJ STRENGTH SEASONAL AND ANNUAL VARIATIONS

```
clear
clc

datapath = '/home/habyarimana/Lucy_revised/';
cd(datapath)

data = load('All_H_value_outside_EEJ_ETHI.txt');

index = find(~isnan(data(:,4)));

H_value_outside_EEJ=  data(index,:);

%% %% Selecting geomagnetically  days in a month based on Kp less or equal to 2

filename=sprintf('kp_index.txt'); % name of file that contains Kp values
Fid=fopen(filename);

fori= 1% loop to count header lines
   Line=fgetl(Fid);
end
Dat=[]; Count=1; % allocating memory for storing kp data
while 1
    Line= fgetl(Fid);
if Line == -1, break, end% end of the line
yyyy = str2num(Line(1:4));
mm = str2num(Line(5:6));
dd = str2num(Line(7:8));
%       Date = str2num(Line(1:8));
     Date = [yyyy mm dd] ;

     Dat1= str2num(Line(10)); Dat2=str2num(Line(12)); Dat3= str2num(Line(14));Dat4=
str2num(Line(16));
     Dat5= str2num(Line(18));Dat6= str2num(Line(20));Dat7= str2num(Line(22));Dat8=
str2num(Line(24));
     Dat0=[Date repelem(Dat1,3) repelem(Dat2,3) repelem(Dat3,3) repelem(Dat4,3)
repelem(Dat5,3) repelem(Dat6,3) repelem(Dat7,3) repelem(Dat8,3)];
Dat=[Dat;Dat0];
end
```

```
Quiet_days = [];
forij = 1:length(Dat)
%      index5 = find(max(Dat(ij,2:25))==2); %Finding a quiet day
    index5 = find(max(Dat(ij,4:27))==2); %Finding a quiet day
if index5==1
Quiet_day = Dat(ij,:);
else
continue
end
Quiet_days = [Quiet_days;Quiet_day];
end

 %% Converting the Quiet days to doy
doys = [];
forih = 1:length(Quiet_days)
   x = datetime(Quiet_days(ih,1),Quiet_days(ih,2),Quiet_days(ih,3));
doy = day(x,'dayofyear');
doys = [doys; doy];
end

Quiet_days_data = [Quiet_days(:,1) doys];

%% Selecting Sq for quiet days and averaging per month

index6 = find(ismember(H_value_outside_EEJ(:,1:2), Quiet_days_data(:,1:2),'rows'));

Required_hourly_values = H_value_outside_EEJ(index6,:);


year = 2010:1:2013;

for ii = 1:length(year)
   index2 = find(Required_hourly_values(:,1)==year(ii));

   H_value_outside_EEJ1 = Required_hourly_values(index2,:);

if mod(year,4)==0
months_ends = [0 31 60 91 121 152 182 213 244 274 305 335 366];
else
```

```
months_ends = [0 31 59 90 120 151 181 212 243 273 304 334 365];
end

All_quiet_daily = [];
forik = 1:length(months_ends(1,:))-1
      index8 = find(H_value_outside_EEJ1(:,2)>months_ends(ik) &
H_value_outside_EEJ1(:,2)<= months_ends(ik+1));
Req_quiet_data_per_month = H_value_outside_EEJ1(index8,:); % monthly mean sqX value

timevec = 0:1:24;
      H_value_outside_EEJ3 = [];
for it = 1:length(timevec)-1
         index3 = find(Req_quiet_data_per_month(:,3)>=timevec(it)
&Req_quiet_data_per_month(:,3)<timevec(it+1));
         H_value_outside_EEJ2 = nanmean(Req_quiet_data_per_month(index3,:));
         H_value_outside_EEJ3 = [H_value_outside_EEJ3;H_value_outside_EEJ2];
end
%        H_value_outside_EEJ3(:,3) = (timevec(:,1:end-1))';

%%--------------------------x component baseline value----------------------
Hx =
[H_value_outside_EEJ3(1,4);H_value_outside_EEJ3(2,4);H_value_outside_EEJ3(3,4);H_value_
outside_EEJ3(24,4)];
   H0x =nanmean(Hx) ;
HOx = ones(24,1)*H0x;

%%------------------- x Hourly departures from baseline----------------
X_Hourly_departures = H_value_outside_EEJ3(:,4) - HOx;
X_Delta_C = ((X_Hourly_departures(1,:)- X_Hourly_departures(24,:)))/23;

   sqX10 = [];
for t=1:1:24
      Sq1 = X_Hourly_departures(t,:)+(t-1)*X_Delta_C;
      sqX10 = [sqX10;Sq1];
end
All_quiet_daily = [All_quiet_daily sqX10];
end
fout = sprintf('/home/habyarimana/Lucy_revised/SqX_Annual/All_annual_sqx%d.txt',year(ii));
dlmwrite(fout, All_quiet_daily,'\t')
end
```

```
clear
clc

datapath = '/home/habyarimana/Lucy_revised/SqH/EEJ_annual_seasonal/';
cd(datapath)

Data1 = load('All_annual_EEJ_data_2010_AAE.txt');
Data2 = load('All_annual_EEJ_data_2011_AAE.txt');
Data3 = load('All_annual_EEJ_data_2012_AAE.txt');
Data4 = load('All_annual_EEJ_data_2013_AAE.txt');

data1 = nanmedian(Data1(2:end,:),2);
data2 = nanmedian(Data2(2:end,:),2);
data3 = nanmedian(Data3(2:end,:),2);
data4 = nanmedian(Data4(2:end,:),2);

t = 1:length(data1);
plot(t,data1,'k',t,data2,'r',t,data3,'b',t,data4,'g')

xlim([0 24])
set(gca,'XTick',[0 3 6 9 12 15 18 21 24]);
ylabel('EEJ (nT)', 'Fontsize',12)
xlabel('LT (Hours)', 'Fontsize',12)

h = legend('2010','2011','2012','2013');
set(h,'Orientation','vertical','box','off','Location','northeast');

saveas(gcf,'Annual-EEJ-AAE.fig');
```

APPENDIX V: A SCRIPT TO PLOT THE STORM TIME VARIATIONS OF THE GEOMAGNETIC FIELD FOR THE SELECTED STORMS IN THE STUDY PERIOD

```
clear
clc

set(0,'DefaultAxesFontSize',12)

datapath1 = '/home/habyarimana/Lucy_revised/SqH/All_sqH_data/';
cd(datapath1)

H_value = load('All_SqH_inside_EEJ_AAE_2013.txt');

%% Selecting the disturbed day
x = datetime(2013,06,01); % yyyy,mm,dd
doy = day(x,'dayofyear');

index1 = find(H_value(:,2)==doy);
Required_sqH_value = H_value(index1,3);

%% Selecting the quietest day of the month
x1 = datetime(2013,06,16); % yyyy,mm,dd
doy1 = day(x1,'dayofyear');
index2 = find(H_value(:,2)==doy1);
Required_sqH_quiet = H_value(index2,3);
%% Solar disturbed variation
sd = Required_sqH_value - Required_sqH_quiet;
plot(sd,'k*-','Linewidth',2)
xlim([0 24])
Ytick = strsplit(num2str(get(gca,'Ytick'))); % Makes the y-tick a whole
number
set(gca,'YTickLabel', Ytick);
set(gca,'XTick',0:4:24,'XTickLabel',{'0','4','8','12','16','20','24'})
xlabel('LT (Hours)')
ylabel('Solar disturbed Variation (nT)')
title('AAE: 2013-06-01')
```